Uric acid treatment after stroke modulates the Krüppel-like factor 2-VEGF-A axis to protect brain endothelial cell functions: impact of hypertension

Elisabet Vila[1], Montse Solé[2], Núria Masip[1], Lídia Puertas-Umbert[1], Sergi Amaro[3,4], Ana Paula Dantas[5], Mercedes Unzeta[2], Pilar D'Ocon[6], Anna Maria Planas[4,7], Ángel Chamorro[3,4], Francesc Jiménez-Altayó[1]*

[1]Departament de Farmacologia, de Terapèutica i de Toxicologia, Facultat de Medicina, Institut de Neurociències, Universitat Autònoma de Barcelona, Bellaterra, Spain. [2]Departament de Bioquímica i de Biologia Molecular, Institut de Neurociències, Universitat Autònoma de Barcelona, Bellaterra, Barcelona, Spain. [3]Comprehensive Stroke Center, Hospital Clínic, University of Barcelona, Barcelona, Spain. [4]Àrea de Neurociènces, Institut d'Investigacions Biomèdiques August Pi i Sunyer (IDIBAPS), Barcelona, Spain. [5]Institut Clínic Cardiovascular, Institut d'Investigacions Biomèdiques August Pi i Sunyer (IDIBAPS), Barcelona, Spain. [6]Departamento de Farmacología, Facultad de Farmacia, Universitat de València, Valencia, Spain. [7]Departament d'Isquèmia Cerebral i Neurodegeneració, Institut d'Investigacions Biomèdiques de Barcelona (IIBB), Consejo Superior de Investigaciones Científicas (CSIC), Barcelona, Spain.

***Correspondence:** Dr F Jiménez-Altayó, Departament de Farmacologia, de Terapèutica i de Toxicologia, Facultat de Medicina, Institut de Neurociències, Universitat Autònoma de Barcelona, 08193 Bellaterra (Cerdanyola del Vallès), Spain. E-mail: francesc.jimenez@uab.cat, Tel: (+34) 93 581 1952; Fax: (+34) 93 581 1953.

ORCID: 0000-0002-9034-2041

Abstract

Uric acid (UA) is a promising protective treatment in ischaemic stroke, but the precise molecular targets underlying its *in vivo* beneficial actions remain unclear. High concentrations of UA inhibit angiogenesis of cultured endothelial cells via Krüppel-like factor 2 (KLF)-induced downregulation of vascular endothelial growth factor (VEGF), a pro-angiogenic mediator that is able to increase blood-brain barrier (BBB) permeability in acute stroke. Here, we investigated whether UA treatment after ischaemic stroke protects brain endothelial cell functions and modulates the KLF2-VEGF-A axis. Transient intraluminal middle cerebral artery (MCA) occlusion/reperfusion was induced in adult male spontaneously hypertensive (SHR) rats and corresponding normotensive Wistar-Kyoto (WKY) rats. Animals received UA (16 mg/kg) or vehicle (Locke's buffer) i.v. at reperfusion. BBB permeability was evaluated by Evans blue extravasation to the brain and in human cerebral endothelial hCMEC/D3 cells under oxygen-glucose deprivation/re-oxygenation. Circulating VEGF-A levels were measured in rats and acute ischaemic stroke patients from the URICO-ICTUS trial. Angiogenesis progression was assessed in Matrigel-cultured MCA. Worse post-stroke brain damage in SHR than WKY rats was associated with higher hyperaemia at reperfusion, increased Evans blue extravasation, exacerbated MCA angiogenic sprouting, and higher VEGF-A levels. UA treatment reduced infarct volume and Evans blue leakage in both rat strains, improved endothelial cell barrier integrity and KLF2 expression, and lowered VEGF-A levels in SHR rats. Hypertensive stroke patients treated with UA showed lower levels of VEGF-A than patients receiving vehicle. Consistently, UA prevented the enhanced MCA angiogenesis in SHR rats by a mechanism involving KLF2 activation. We conclude that UA treatment after ischaemic stroke upregulates

KLF2, reduces VEGF-A signalling, and attenuates brain endothelial cell dysfunctions leading to neuroprotection.

Keywords: hypertension; ischaemic stroke; Krüppel-like factor 2; vascular endothelial growth factor-A; blood-brain barrier; angiogenesis

1. Introduction

Endothelial cells form a single layer that covers the inner lining of the blood vessels, known as vascular endothelium. Brain endothelium modulates multiple functions, including cerebral vessel tone, blood-brain barrier (BBB) function, and neovascularization, which are critical to maintaining brain homeostasis. During ischaemic stroke, the integrity of the brain endothelium is perturbed, resulting in endothelial cell release of proinflammatory mediators, degradation of the vascular basement membrane, BBB breakdown, and altered neovascularization/angiogenesis [1]. After stroke, angiogenesis, the outgrowth of new vessels from preexisting blood vessels, promotes survival of the resilient cells, acts to remove injured tissue and facilitates the adequate environment for neurogenesis [[2], [3], [4]]. Hypertension is the leading cause of stroke and leads to larger brain damage and worse functional outcomes [5,6]. It is proposed that the angiogenic response in hypertension may be dysfunctional impairing recovery [3,7]. However, in hypertension, the knowledge of the progression and the pathophysiological relevance of altered brain endothelium functions, namely BBB disruption and altered neovascularization, is limited.

Endovascular thrombectomy and/or intravenous administration of recombinant tissue-type plasminogen activator (rtPA) are the only effective treatments currently available for ischaemic stroke patients, thus, development of novel therapeutic strategies is a subject of utmost importance [8]. The vascular endothelial growth factor (VEGF) family of angiogenic growth factors is implicated in neuroprotection, neurogenesis, and angiogenic growth [4]. Upregulation of VEGF occurs after a few hours in response to ischaemic stroke [9,10], both in the penumbra area [9,11] and in cortical areas functionally related to the area of the infarction [12]. Among them, the human VEGF-A is a Janus-faced molecule, since together with its proangiogenic and neuroprotective effects, it disrupts the BBB integrity, leading to edema, hemorrhage, and brain damage [[4], [13], [14], [15]]. Therefore, fine-tune regulation of VEGF-A signalling to protect early BBB opening and associated brain injury may be a feasible target of acute ischaemic stroke therapy [16,17].

Uric acid (UA) treatment has shown to be safe and neuroprotective in both experimental [[18], [19], [20], [21], [22], [23], [24], [25]] and human [[26], [27], [28], [29], [30]] ischaemic stroke. Although the mechanisms underlying UA beneficial actions are not completely understood, it is proposed that the brain vasculature could be an important target of this therapy [[21], [25], [31]]. Interestingly, a previous study showed that high concentrations of UA inhibit angiogenesis of cultured endothelial cells via Krüppel-like factor 2 (KLF2)-induced negative regulation of VEGF-A expression [32]. KLF2 is a member of the zinc finger family of transcription factors that modulates essential cellular functions, including regulation of endothelial cell growth, differentiation and activation [33]. Further, KLF2 expression can be amplified either by blood flow-induced shear stress [34,35] or by statins [36,37], effects that are mediated

through the activation of the extracellular-signal-regulated kinase 5 [[37], [38], [39]]. KLF2 protects mice from thrombus formation by a mechanism involving decreased expression of endothelial thrombotic factors [40]. Notably, Shi et al. [41] elegantly described that brain infarction and BBB permeability were enhanced in the absence of KLF2 and attenuated after its overexpression, which is the first direct evidence of a protective role of KLF2 in ischaemic stroke.

The main objective of the present study was to investigate whether protection of brain endothelial cell functions and modulation of the KLF2-VEGF-A axis are involved in UA-induced beneficial actions in a model of ischaemia/reperfusion in spontaneously hypertensive rats (SHR) and their control rats (WKY). The results show that worse brain damage in SHR rats is associated with higher BBB disruption and exacerbated middle cerebral artery (MCA) angiogenic sprouting. UA treatment early after stroke protected BBB function in both rat strains and abolished the increased angiogenic responses in SHR rats. Notably, the antiangiogenic effects of UA in hypertension were at least partly mediated by KLF2, and were associated with a decrease in circulating levels of VEGF-A. Accordingly, hypertensive ischaemic stroke patients treated with UA in the acute phase of stroke showed reduced serum VEGF-A levels compared with placebo treated patients. Overall, the findings demonstrate that UA treatment after stroke leads to protection of brain endothelial cell functions, an effect that is associated with upregulation of KLF2 and reduction of VEGF-A signalling.

2. Materials and Methods

2.1. Animals

Twelve- to 14-wk-old male WKY (n = 54) and SHR (n = 78) rats (Janvier, Madrid, Spain) were housed under controlled environmental conditions of temperature and humidity, a 12:12-h light-dark cycle, and provided with free access to food and water before and after surgery. All of the experiments were carried out under the Guidelines established by the Spanish legislation (RD 1201/2005) and according to the Guide for the Care and Use of Laboratory Animals, published by the United States National Institutes of Health (NIH Publication 85-23, revised 1996). Experiments were approved by the Ethics Committee of the Universitat Autònoma de Barcelona (7944/B-RP-042/16) and were carried out in compliance with the European legislation.

2.2. Patients

Patient serum samples were obtained from the population included in the URICO-ICTUS study (NCT00860366), a double-blind, multicenter, randomized, placebo-controlled, phase-2b/3 trial where 411 alteplase-treated patients were randomized to receive UA 1000 mg or placebo before the end of alteplase infusion [26]. In brief, the URICO-ICTUS trial included patients with acute ischaemic stroke treated with alteplase within 4.5 h of clinical onset at ten Spanish Stroke Centers between July 1, 2011, and April 30, 2013. Overall, 211 patients were treated with UA and 200 patients were treated with placebo. The main results and detailed methods of the URICO-ICTUS trial are available elsewhere [26]. Approval was obtained from all ethical boards of the participating centers and all participants (or their legal representatives) provided written informed consent. Human serum studies were carried out according to the Institutional Clinical Review Board of Spanish clinical centers, and the patients' written consent conformed to the ethical guidelines of the 1975 Declaration of Helsinki.

2.3. Transient Middle Cerebral Artery Occlusion

Intraluminal occlusion (90 min) of the right MCA with reperfusion (30 min or 24 h) was induced in rats anaesthetized with isoflurane (3.5%; IsoFlo®, Laboratotios Dr. Esteve SA, Barcelona, Spain) vaporized in O_2 and N_2O (30:70; Air Liquide España SA, Barcelona, Spain) to induce focal brain ischaemia [21]. Sham-operated (sham) rats were subjected to all the surgical procedures and were used as controls. Continuous monitoring of cortical cerebral blood flow (CBF; laser Doppler flowmetry system; Perimed AB, Järfalla, Sweden) was performed as reported [21]. Briefly, a guide was implanted on a thinned-skull cranial window (stereotaxic coordinates: 2 mm posterior and 3.5 mm lateral to Bregma) created in anaesthetised rats the day before ischaemia. Before induction of ischaemia, the laser Doppler probe was introduced through the guide and registration was started. Body temperature was monitored with a rectal probe and controlled at 37 ± 0.5 °C during surgery with a heating blanket connected to a temperature-control system (Cibertec, Madrid, Spain).

120 mins after MCA occlusion (i.e. after 30 min of reperfusion), rats received an intravenous infusion of UA (16 mg/kg; Sigma-Aldrich, St. Louis, MO, USA) or vehicle (Locke's buffer), and were studied after 24 h of reperfusion. This dose was chosen based upon previous studies showing a neuroprotective effect of UA in stroke [[18], [19], [20], [21], [22], [23], [24], [25]]. A nine-point scale (0 = no deficit to 9 = highest handicap) neurological test was performed at 24 h of reperfusion [42]. Afterwards, animals were deeply anaesthetized with isoflurane (5%) immediately prior to euthanasia by decapitation. The brain was removed and infarct volume was assessed in 2-mm-thick coronal sections stained with 2,3,5-triphenyltetrazolium chloride (5%; Sigma-Aldrich) staining, as described [43].

Animals were randomly allocated to the following experimental groups: a) sham surgery was applied to rats that received vehicle, including normotensive rats (sham WKY + vehicle, n = 5) and hypertensive rats (sham SHR + vehicle, n = 6); and b) I/R was induced in normotensive or hypertensive rats that received either vehicle (I/R WKY + vehicle, n = 11; I/R SHR + vehicle, n = 13) or UA (I/R WKY + UA, n = 10; and I/R SHR + UA, n = 10). Ten animals were excluded from the study following these criteria: technical surgical problems (n = 2 WKY; n = 6 SHR) and unsuccessful CBF registry (n = 2 WKY). For plasma VEGF-A studies, an additional set of rats subjected to ischaemia followed by 24 h of reperfusion was used: sham WKY + vehicle, n = 8; sham SHR + vehicle, n = 12; I/R WKY + vehicle, n = 5; I/R SHR + vehicle, n = 5; I/R WKY + UA, n = 5; and I/R SHR + UA, n = 6). Eight animals were excluded from the study following these criteria: technical surgical problems (n = 5 SHR) and unsuccessful CBF registry (n = 1 WKY; n = 2 SHR).

Additional groups of untreated rats were studied after ischaemia and 30 min of reperfusion, including normotensive (WKY I/R, n = 5) and hypertensive (SHR I/R, n = 12) rats. One animal was excluded from this study due to technical surgical problems (n = 1 SHR).

2.4. Blood Pressure Measurements

Measurement of systolic blood pressure (SBP) was carried out in a blinded fashion in conscious SHR and WKY rats using the tail-cuff method (NIPREM 645; Cibertec, Madrid, Spain). To make the pulsation more detectable, rats were restrained for 10-15 min in a dark and warm cage followed by several cycles of inflation/deflation to

measure blood pressure. Rats were allowed to habituate to the procedure for 3 days before doing the final measurement the day before surgery. The average SBP of each rat was determined from six consecutive measurements.

2.5. Analysis of circulating levels of VEGF-A

Blood (500 µl) was collected intracardially just before rats were killed. Plasma circulating levels of VEGF-A were measured in a 96-well plate using a Milliplex MAP rat RECYTMAG-65K Magnetic Bead Panel (Merck Millipore, Burlington, MA, USA) following the kit-specific protocols, as described [21]. Analytes were quantified with xPONENT 4.2 software for MagPix (Luminex, Austin, TX, USA).

Serum VEGF-A levels were measured in serum samples obtained before the onset of thrombolytic therapy and following 6-12 h in a subset of 56 acute ischaemic stroke patients included in the URICO-ICTUS trial (27 allocated to receive UA, 29 allocated to receive placebo) [26]. Serum VEGF-A levels were determined using an enzyme-linked immunosorbent assay (Abcam, Cambridge, UK) according to the manufacturer's instructions.

2.6. Evans blue BBB permeability

Evans blue extravasation to the brain tissue was studied as a measure of BBB permeability, as reported [43,44]. Briefly, Evans blue (2% in saline; Sigma-Aldrich) was administered i.v. (80 mg/kg of body weight) 22 h after ischaemia in rats anaesthetized with isoflurane (3.5%) vaporized in O_2 and N_2O (30:70). Two hours later, the animals were perfused through the heart with saline. The brain tissue was removed and sliced in 2-mm-thick coronal sections to measure the volume of tissue with Evans

blue extravasation. Images of the sections were scanned and analyzed with Image J software (National Institutes of Health, Bethesda, MD, USA). All measures involving Evans blue permeability were performed blinded to all experimental conditions.

2.7. *In vitro* OGD and permeability in human hCMEC/D3 endothelial cells

The human cerebral microvascular endothelial cell line hCMEC/D3 was obtained from Dr. Couraud's laboratory in Paris, France [45,46], and were used between passages 27 and 35. Cells were cultured on 150 μg/mL collagen type I (Rat tail, Corning, NY, USA)-coated plates, in endothelial basal medium-2 (Lonza, Barcelona, Spain) supplemented with 5% fetal bovine serum (FBS, Life Technologies, Madrid, Spain), 1.4 μM Hydrocortisone (Sigma-Aldrich), 5 μg/mL Ascorbic Acid (Sigma-Aldrich), 1% Chemically Defined Lipid Concentrate (Life Technologies), 10 mM HEPES (Life Technologies) and 1 ng/mL human Fibroblast Growth Factor-basic (Sigma-Aldrich). Cells were maintained at 37 ºC, in a humidified atmosphere containing 5% CO_2. For permeability assays, cells were seeded at 1,000,000 cells/mL in collagen and fibronectin-coated 12-well Transwell inserts (Transwell polyester membrane inserts, pore size 0.4 μM. Corning, NY, USA) and allowed to grow for 4 days before applying any treatment.

Oxygen and glucose deprivation (OGD) and re-oxygenation were performed as described in Sun *et al*. [47]. Briefly, cells were washed with glucose-free phosphate-buffered saline, and then placed in FBS-free Dulbecco's Modified Eagle's Medium (DMEM, Life Technologies) containing UA (10-1000 μM) or UA (50 μM) plus the highly specific extracellular-signal-regulated kinase 5/KLF2 pathway inhibitor XMD8-92 (1-30 μM) [39,48] into a temperature-controlled (37 ºC) *in vivo* hypoxia workstation

(RUSKINN Sanford, ME, USA), with a gas mixture composed of 5%CO_2, 95% N_2 and 0.5% O_2. Cells were maintained under OGD conditions for 16 h. In parallel, control cells were maintained in FBS-free DMEM containing 5 mM Glucose in an incubator under normoxic conditions (5% CO_2/95% air) for the same time. For re-oxygenation, cells that had undergone OGD were returned to normoxic conditions after addition of glucose (5 mM) to the media for 24 h.

After OGD and re-oxygenation, endothelial cell permeability was determined by measuring the pass of dextran from the luminal to the abluminal side of the insert, as described [49]. Briefly, 500 µL of phenol red-free DMEM containing 2 mg/mL 70 kDa Fluorescein isothiocyanate-dextran (Sigma-Aldrich) were added replacing the luminal side culture media. The permeable filter inserts were then sequentially transported at 5 min intervals for 30 min in total into new wells containing pre-warmed phenol-free DMEM, maintaining cells at 37 ºC during the process. Then, fluorescence of each well (two replicates per experimental condition) was measured at 485 nm and 520 nm (ex/em), and apparent permeability coefficients (cm/sec) were calculated from curves slopes (fitted using linear regression) obtained by plotting cumulative volume cleared against time, for each experimental condition. Permeability values were normalised for non-treated OGD/re-oxygenation or non-treated normoxia average values.

2.8. MCA angiogenesis

MCA angiogenic growth was measured following the protocol described by Vicente *et al*. [50]. MCA were isolated at 24 h or at 30 min after reperfusion and measurements of angiogenesis were performed after culture day 4. In preliminary experiments, we observed that the MCA did not show angiogenic growth after isolation at 24 h, and

neovessel formation was not evident enough until day 4. Briefly, segments of the right (ischaemic) and left (contralateral to ischaemia) MCA were dissected under a surgical microscope, kept in cold Krebs-Henseleit solution (KHS; composition in mM: NaCl 112.0; KCl 4.7; $CaCl_2$ 2.5; KH_2PO_4 1.1; $MgSO_4$ 1.2; $NaHCO_3$ 25.0 and glucose 11.1) supplemented with amphotericin B (15 mg/l) (Biowhittaker ®, Lonza, Basel, Switzerland) and gentamicine (30 mg/l) (Genta-gobens ®, Laboratorios Normon SA, Tres Cantos, Madrid, Spain), and gassed with 95% O_2 and 5% CO_2. Afterwards, vessels were immersed into the wells of a 96-well plate (Costar, Corning Inc., Corning, NY, USA) containing Matrigel® (50 µl; BD Bioscience, San Jose, CA, USA) at 4 ºC. After 30 min at room temperature, 200 µl of microvascular endothelial cell growth medium (Labclinics, Barcelona, Spain) supplemented with fetal bovine serum (5%), amphotericin B (15 mg/l) and gentamicine (30 mg/l) were added to each well. Plates were incubated at 37 °C and 5% CO_2 for 14 days, and culture medium was renewed the day after seeding and every two days.

Neovessel growth progression was measured in MCA from WKY and SHR rats subjected to ischaemia (90 min)/reperfusion (24 h) and treated with UA or vehicle. Furthermore, ischaemia (90 min)/reperfusion (30 min) was induced in a separate set of WKY and SHR rats and ischaemic MCA segments were exposed *ex vivo* to either UA (10-30 µM), the KLF2 expression inductors simvastatin (10 µM) [51] and suberoylanilide hydroxamic acid (SAHA; 10 µM) [52], XMD8-92 (5 µM), and the corresponding vehicles (Locke's buffer or 0.1% DMSO), added into the culture medium for 23.5 h to study MCA angiogenesis. The concentrations of UA (10 and 30 µM) were chosen based on plasma concentrations (4-5 µg/ml; i.e. 24-30 µM) reached after i.v. administration (16 mg/kg) in ischaemic rats [21]. Angiogenic growth images were taken

the fourth, fifth, sixth, seventh, tenth and fourteenth day after seeding. Image capture was performed using an inverted microscope equipped with a camera (10x objective; TE2000 Nikon Eclipse-S, Nikon España, Madrid, Spain). The length of the longest vessel sprouting from the outer surface of the MCA (starting point) was measured with Image J software (National Institutes of Health, Bethesda, MD, USA) [50]. A minimum of three fields per MCA segment were measured and the average recorded.

2.9. Western blot

Human cerebral microvascular endothelial cells hCMEC/D3 were homogenized in 50 mM Tris-HCl (pH 7.5), containing 1% Triton X-100, 10 mM EDTA and a protease inhibitors cocktail (1:100; Sigma-Aldrich), and were then sonicated for 10 seconds. Protein concentration in homogenates was determined by the Bradford method, and equal amounts of protein (20 μg/lane) were separated by SDS-PAGE and transferred onto nitrocellulose membranes, as described [47]. Primary antibodies used were anti-KLF2 (1:500; #Ab203591, lot GR313218-2, Abcam), anti-occludin 1 (1:2000; #33-1500, lot QD215073, Thermo Fisher Scientific, Carlsbad, CA, USA), anti-ZO 1 (1:1000; # 44-2200, lot 1574917A, Thermo Fisher Scientific), anti-Claudin 5 (1:500; #sc-374221, lot H0516, Santa Cruz Biotechnology, Dallas, TX, USA), anti-VE-cadherin (1:500; #sc-9989, lot A1217, Santa Cruz Biotechnology) and anti-β-Actin (1:20000; #A1978, Sigma-Aldrich). Secondary HRP (horseradish peroxidase)-conjugated antibodies used were anti-rabbit IgG (1:1,000; BD Biosciences, San Jose, CA, USA) and anti-mouse IgG (1:1000; Dako, Madrid, Spain). Band intensities were quantified with ImageJ software, and relativized using β-Actin as a loading control. The values were then normalised for non-treated cells in normoxia.

2.10. Quantitative Real-Time PCR (qRT-PCR)

Branches of the MCA and the remaining cerebral arteries were dissected, were kept at -70 °C, and used for mRNA expression analysis. mRNA levels were determined by SYBER green-based qRT-PCR detection following the manufacturer's guidelines (Thermo Fisher Scientific), as described [53]. Amounts of VEGF-A, VEGF receptor 2 (VEGFR2), and KLF2 mRNA were normalised relative to the expression of internal controls GAPDH and 18S ribosomal RNA. Cycle threshold (Ct) values were referenced to the average Ct of internal controls [comparative Ct (ΔCt)] and were converted to the linear form relative to corresponding levels in control sham vessel levels ($2^{-\Delta\Delta Ct}$).

2.11. Immunofluorescence

Segments of the ipsilateral MCA from SHR rats subjected to ischaemia (90 min)/reperfusion (30 min) were exposed *ex vivo* to either vehicle or UA (30 μM) added into the culture medium for 23.5 h. Afterwards, segments were fixed in 4% paraformaldehyde and embedded in Tissue Tek OCT embedding medium (Sakura Finetek Europe, Zoeterwoude, the Netherlands), frozen in liquid nitrogen and kept at −70 °C. Frozen transverse sections (14 μm-thick) were incubated for 1 h with anti-KLF2 (1:100; #Ab203591, lot GR313218-2, Abcam) primary antibody in a humidified chamber at 37 °C. After several rinses, sections were incubated (for 45 min) with a donkey anti-rabbit IgG secondary antibody conjugated to Cyanine 3 (1:200; #711-165-152, lot 110351, Jackson ImmunoResearch Laboratories, West Grove, PA, USA) in a humidified chamber at 37°C. Sections were processed for immunofluorescence staining as previously described [21]. The specificity of the immunostaining was verified by omission of the primary antibody. Images were captured using a FV1000 confocal microscope (Olympus Iberia, Barcelona, Spain). Quantitative analysis of

average fluorescence signal was obtained in at least two rings of each animal with Image J software (National Institutes of Health, Bethesda, MD, USA), and the results were expressed as arbitrary units.

2.12. Statistical Analysis

Results are expressed as mean ± SEM of the number (n) of rats indicated in the figure legends. Normal distribution was checked before choosing the appropriate statistical analysis. Comparison between two groups was carried out with the Mann-Whitney or Student's t test. Comparison between more than two groups (one single factor) was carried out with one-way ANOVA or the Kruskal-Wallis test followed by Tukey's or Dunn’s post-test, respectively. Difference in angiogenic growth between normotensive and/or hypertensive rats and the effect of UA treatment were assessed by a repeated measures two-way ANOVA with Bonferroni's post-test for grouped analyses. Data analysis was carried out using GraphPad Prism version 5 software (La Jolla, CA, USA). Serum VEGF-A levels in patients were reported as median with interquartile ranges and compared with the Mann-Whitney test, and were subsequently transformed to the cubic root to approach normality before their inclusion in general linear models constructed to assess the impact of UA vs. placebo on longitudinal levels of VEGF-A according to premorbid hypertension status. A value of $P < 0.05$ was considered significant.

3. Results

3.1. UA treatment is neuroprotective in ischaemic WKY and SHR rats

SBP was higher ($P < 0.001$) in SHR (168.41 ± 1.60 mmHg; n = 17) than WKY (128.23 ± 2.60 mmHg; n = 18) rats, as expected. After occluding the MCA for 90 min, the rats received (i.v.) either UA or vehicle (Locke's buffer) 120 min after occlusion (i.e. 30 min after reperfusion onset) (Fig. 1A). The decrease of CBF during ischaemia was comparable among groups (Table 1). However, the increase of CBF at reperfusion was higher in SHR compared to WKY rats (Table 1). After 24 h of reperfusion, larger ($P < 0.01$) cortical infarct volumes were observed in vehicle-treated hypertensive compared to normotensive ischaemic rats (Fig. 1B and C). A single dose administration of UA reduced ($P < 0.01$) the cortical infarct volumes in both WKY (Fig. 1B) and SHR (Fig. 1C) rats. The neurological score was similar in vehicle-treated SHR compared to WKY ischaemic rats (Fig. 1B and C). UA treatment did not significantly decrease neurological score values in WKY or SHR rats after separate analysis of each strain. However two-way ANOVA by treatment and strain factors showed a global significant improvement of the neurological score in the rats that received UA ($P < 0.01$; two-way ANOVA; Fig. 1D).

3.2. UA treatment protects the BBB integrity in ischaemic WKY and SHR rats

BBB permeability was assessed by Evans blue extravasation to the brain parenchyma. In a separate set of rats, the MCA was occluded for 90 min and the rats received (i.v.) either UA or vehicle 30 min after reperfusion onset. Evans blue was administered (i.v.) at 22 h of reperfusion and the volume of Evans blue extravasation to the brain parenchyma was measured at 24 h of reperfusion (Fig. 2A). Evans blue extravasation was larger ($P < 0.01$) in vehicle-treated SHR compared to WKY ischaemic rats (Fig. 2B). Treatment with UA significantly attenuated ($P < 0.05$) Evans blue extravasation in both rat strains.

3.3. UA treatment inhibits the exacerbated MCA angiogenic response in ischaemic SHR rats

A previous study suggested that high concentrations of UA inhibit angiogenesis of cultured endothelial cells [32], then, our next step was to study whether UA exerted similar actions in ischaemic stroke. In the present work, we studied the angiogenic response of isolated MCA from WKY and SHR rats that were previously subjected to cerebral ischaemia (90 min)/reperfusion (24 h), and treated (i.v.) with either UA or vehicle 30 min after reperfusion onset (Fig 3A). The ipsilateral to ischaemia (ischaemic) and contralateral MCA was cultured in growth medium containing Matrigel, and the angiogenic growth was longitudinally scored at day 4, 5, 6, 7, 10 and 14 after seeding (Fig 3A). Hypertension did not modify the MCA angiogenic response in sham rats (Fig 3B and C). Neither ischaemia/reperfusion, nor UA treatment modified angiogenic growth in the contralateral MCA (results not shown). In the ipsilateral MCA, neovessel sprouting was similar in vehicle-treated ischaemic compared to sham WKY rats (Fig 3B and C). In contrast, vehicle-treated ischaemic SHR rats showed an early-term (from day 4 to 7) increase in neovessel formation compared to either sham SHR rats or ischaemic WKY rats (Fig 3C). This higher MCA angiogenic growth in ischaemic SHR rats stopped at day 10 and was lower ($P < 0.05$) at day 14 (WKY: 594.5 ± 38.3 μm; SHR: 482.4 ± 34.8 μm) compared to ischaemic WKY rats (Fig 3C). Although UA treatment did not significantly modify neovessel sprouting after ischaemia in WKY rats (Fig 3D), it prevented the early exaggerated angiogenic response in SHR animals (Fig 3E).

3.4. UA treatment decreases circulating levels of VEGF-A in ischaemic SHR rats and in hypertensive acute ischaemic stroke patients

The antiangiogenic actions of UA in cultured endothelial cells are mediated via the KLF2-VEGFA axis [32]. To evaluate the involvement of this signalling pathway on the neuroprotective activity of UA in ischaemic stroke, we first studied the circulating levels of VEGF-A in WKY and SHR animals subjected to cerebral ischemia (90 min)/reperfusion (24 h) (Fig. 4A). Plasma levels of VEGF-A were significantly higher ($P < 0.05$) in vehicle-treated ischaemic SHR, but not WKY, rats compared to sham rats. Treatment with UA avoided the increase in the circulating VEGF-A levels observed in vehicle-treated SHR rats after I/R (Fig 4A).

We, subsequently, tested the translational value of these findings by measuring serum VEGF-A levels in acute ischaemic stroke patients from the URICO-ICTUS trial [26]. The general traits of the included population according to hypertension history and treatment allocation (UA vs. placebo) are shown in Table 2. Overall, pre-treatment VEGF-A levels were similar in both groups according to treatment allocation [median (IQR) 214 (123-368) pg/ml for placebo group vs. 211 (99 – 318) pg/ml for UA group, Mann-Whitney test $P = 0.549$] and to premorbid hypertension [median (IQR) 222 (112 – 386) pg/ml for hypertensive patients vs. 192 (97 – 282) pg/ml for no hypertensive patients, Mann-Whitney test $P = 0.235$]. In linear regression models, a significant interaction was found between treatment allocation (UA vs. placebo therapy) and premorbid hypertension status on the prediction of serum cubic-root transformed VEGF-A levels at 6-12 h ($P = 0.05$). In comparison with placebo, in the subgroup of patients with pre-treatment hypertension, the administration of UA was associated with significantly lower levels of cubic-root transformed VEGF-A at 6-12 h (Exp{B} = 0.138,

95% confidence interval 0.029-0.653, *P* = 0.012), whereas no effect was apparent in the subgroup of patients without pre-treatment hypertension (Exp{B} = 1.281, 95% confidence interval 0.377-4.355, *P* = 0.691). The distribution of serum VEGF-A levels according to treatment allocation and history of hypertension is shown in Fig. 4B. Circulating VEGF-A levels were significantly reduced ($P < 0.05$) after 6-12 h of combined treatment with UA and rtPA in hypertensive, but not normotensive, stroke patients.

3.5. UA treatment increases genic expression of KLF2 in cerebral vessels from ischaemic SHR rats

It is known that KLF2 can inhibit angiogenesis through downregulation of either the potent pro-angiogenic factor VEGF-A [32] or VEGFR2 [54] expression. We assessed mRNA levels of VEGF-A, VEGFR2 and KLF2 in cerebral arteries from WKY and SHR rats subjected to cerebral ischaemia (90 min)/reperfusion (24 h) and treated (i.v.) with either UA or vehicle (Fig 5). VEGF-A and VEGFR2 mRNA levels were not altered neither by I/R nor by UA treatment in WKY and SHR animals. However, in the same vessels, genic expression of KLF2 was significantly increased by UA treatment in SHR but not in WKY animals.

3.6. KLF2 inhibition does not prevent the reduction of BBB permeability induced by UA

To study the mechanisms by which UA protects the BBB, we cultured human cerebral microvascular endothelial hCMEC/D3 cells to create an *in vitro* BBB [49]. We subsequently subjected the cells to 16 h of OGD followed by 24 h of re-oxygenation, and the permeability was assessed by measuring fluorescein isothiocyanate dextran

passage (Fig 6A). As expected, exposure of non-treated cells to OGD + re-oxygenation induced an increase ($P < 0.001$) in BBB permeability (Fig 6B), an effect that was not accompanied by changes in protein expression of neither tight junction proteins occludin, zonula occludens-1 and claudin-5, nor adherens junction protein VE-cadherin (Fig 6C). Notably, UA significantly attenuated the permeability of the barrier under OGD + re-oxygenation conditions (Fig 6B). Previous studies reported that KLF2 protects BBB function [41,55]. In hCMEC/D3 cells, KLF2 expression was significantly attenuated ($P < 0.05$) after OGD + re-oxygenation, an effect that was prevented by UA (Fig 6D). However, incubation with XMD8-92 (1-30 μM), a highly specific extracellular-signal-regulated kinase 5/KLF2 pathway inhibitor, did not prevent the BBB-protective effects of UA (Fig 6E).

3.7. The KLF2-VEGF-A axis mediates the antiangiogenic actions of UA and modulates angiogenic activity in ischaemic vessels

To determine the involvement of KLF2 on the antiangiogenic activity showed by UA *in vivo* treatment in ischaemic SHR rats, we studied the direct effects of UA incubation on the MCA angiogenic growth in rats subjected to cerebral ischaemia (90 min)/reperfusion (30 min) (Fig 7A). In these studies, the decrease of CBF during ischaemia was comparable among groups, and the increase of CBF at reperfusion was higher ($P < 0.01$) in SHR compared to WKY rats (Table 3). Incubation in the culture medium with two different concentrations of UA (10 μM and 30 μM) significantly attenuated MCA neovessel sprouting in both WKY (Fig 7B) and SHR (Fig. 7C) rats. UA (30 μM) incubation in the culture medium tended ($P = 0.065$) to increase KLF2 expression in MCA from ischaemic SHR rats, an effect that was predominantly observed in nuclei from adventitia and arachnoid membrane (Fig 7D). XMD8-92 (5 μM)

reverted ($P < 0.05$) the UA (30 μM)-induced attenuation of MCA neovessel formation (Fig 7E). The effects of two known KLF2 activators, simvastatin (10 μM) and SAHA (10 μM) were assessed by their addition into the culture medium. Both KLF2 activators induced a significant decrease of MCA angiogenic growth that started in the first days after seeding (Fig 7F).

4. Discussion

UA is a promising drug to treat cerebral ischaemic stroke, but the precise mechanisms underlying its beneficial actions remain unclear. In the present work, we show that UA treatment exerts neuroprotective effects after ischaemic stroke in normotensive (WKY) and hypertensive (SHR) rats, as shown by the lower infarct volume and neurological score. In addition, UA prevents the exaggerated angiogenic response observed after stroke in the MCA from SHR rats and protects BBB function. Mechanistically, the UA beneficial actions were associated with modulation of VEGF-A levels and KLF2 expression, a signalling pathway that is strongly disrupted after hypertensive stroke. Together, these findings demonstrate that brain endothelial cell dysfunctions after stroke are a target of UA neuroprotective therapy, and suggest that UA-mediated modulation of the KLF2-VEGF-A axis contributes to this neuroprotection.

In humans, serum levels of VEGF increase in acute ischaemic stroke in association with infarction volume and clinical disability [56,57]. Our results show a similar increase in SHR, but not in WKY, rats after transient MCA occlusion. The clinical significance of acute rises in plasma VEGF levels is under debate, and can either predict good clinical prognosis [57] or can be positively associated with neurological severity in

cardioembolic infarction patients [58]. In the present study, UA neuroprotective treatment normalised the increased circulating VEGF-A levels in the ischaemic stroke model of mechanical thrombectomy in SHR rats, and reduced VEGF-A levels in hypertensive acute ischaemic stroke patients from the URICO-ICTUS trial [26]. In contrast, this VEGF-A reducing effect was not observed neither in ischaemic WKY rats nor in normotensive acute ischaemic stroke patients. Therefore, our study suggests that VEGF-A downregulation during the acute phase of ischaemic stroke is linked to neuroprotection only among hypertensives.

Modulation of stroke-responsive cerebral transcription factor expression is a promising tool for the treatment of ischaemic stroke [59,60]. Among them, KLF2 is a transcription factor that modulates VEGF-A signalling exhibiting a complex activity depending on the context. Previous evidence indicates that KLF2 counteracts angiogenic VEGF-A activity either through inhibition of VEGFR2 expression [54] or by directly binding to the VEGF-A promoter region [32]. Furthermore, KLF2 inhibits angiogenesis by other signalling pathways such as inhibition of hypoxia-inducible factor-1 [61]. Interestingly, a previous study showed that UA reduces angiogenesis of cultured endothelial cells via KLF2-induced negative regulation of VEGF-A expression [32]. In the present work, we show that UA strongly increases gene expression for KLF2 in cerebral vessels from SHR, but not in WKY, rats after 24 h of reperfusion, an effect that is not coupled by changes in VEGF-A or VEGFR2 gene expression. Thus, our results cannot establish the exact mechanism by which UA-mediated increases in KLF2 expression may affect the VEGF-A signalling pathway, and therefore further studies would be necessary. Notably, to gain further insight into potential physiological relevance of UA neuroprotective effects and the role of the KLF2-VEGF-A pathway, we next studied the

ex vivo progression of post-stroke MCA angiogenic sprouting. The results show that neovessel formation within a few days (i.e. from day 4 to 7) after seeding is enhanced in MCA from SHR compared to WKY rats after ischaemia/reperfusion. This hypertension-related effect was followed by a late stage (14 days) vessel pruning. These results mirrored those from Yang et al [62] that observed an increased rate of early (3 and 5 days post stimulation) angiogenesis followed by late (10 and 25 days post stimulation) vessel pruning in mesenteric microvascular networks from SHR compared to WKY rats.

Angiogenesis is important to enhance oxygen and nutrient supply to the ischaemic brain tissue [63]. However, new vessels that proliferate within a few days after a stroke [64] may be dysfunctional [65] due to the presence of a modified environment during the acute phase after the ischaemic insult. We suggest that increased levels of VEGF-A early after hypertensive strokes might contribute to promote microvascular dysfunction, an effect that may hamper recovery. In the present study, data collected from either *in vitro* or *in vivo* UA exposure revealed that this drug, at concentrations/doses relevant in stroke therapy, prevents the augmented neovessel formation in MCA from ischaemic SHR rats. In addition, UA diminished the exaggerated MCA angiogenic growth observed in WKY rats after shortening the duration of reperfusion to 30 min. Furthermore, we demonstrate that UA effects on angiogenesis were mediated via KLF2, since either activation or inhibition of this transcription factor emulated or prevented, respectively, the antiangiogenic actions of UA. Nonetheless, we cannot discard that the protective effect of UA on brain infarction might indirectly contribute to its antiangiogenic effects. Noteworthy, the KLF2 activators used in the present study (i.e. simvastatin and SAHA) reduce brain damage in several

experimental models of stroke [[66], [67], [68]], which in combination with the present findings suggests that effective neuroprotective strategies in stroke might converge into the activation of the KLF2 pathway.

BBB breakdown worsens ischaemic brain damage and KLF2 overexpression reduces the size of the lesion and improves BBB function in a normotensive mouse model of acute ischaemic stroke [41]. Although some evidence suggests that hypoxia transiently upregulates KLF2 expression in human umbilical vein endothelial cells [69,70], re-oxygenation following hypoxia reduces KLF2 expression in primary human brain microvascular endothelial cells [70] and in endothelial hCMEC/D3 cells of our study; an effect that can contribute to the observed BBB permeability increase. UA treatment attenuated Evans blue leakage to the brain tissue in WKY and SHR rats after transient ischaemia and decreased the permeability of endothelial hCMEC/D3 cells exposed to hypoxia/re-oxygenation; the latter effect was paralleled by amelioration of KLF2 expression confirming the results obtained in cerebral arteries. Furthermore, the BBB-protective effects of KLF2 have been linked to overexpression of the endothelial cell tight junction factor occludin [[41], [55], [71]]. Although we did not observe alterations in occludin or in other tight and adherens junction protein expression, we could not exclude potential changes on their cellular distribution. In addition, other processes regardless of tight and adherens junction expression/distribution might be involved in BBB opening. Thus, enhanced transendothelial trafficking [72,73], opening of endothelial connexin-43 hemichannels [74] and endothelial cell degeneration [72,75] have also been involved in BBB breakdown. Notably, KLF2 inhibition did not prevent the reduction of permeability induced by UA, suggesting that other mechanisms could also participate in the beneficial actions of this drug on BBB permeability.

In conclusion, the present study demonstrates that UA treatment after acute ischaemic stroke modulates the KLF2-VEGF-A axis and attenuates brain endothelial cell dysfunctions leading to neuroprotection. These findings extend the neuroprotective actions of uric acid [[18], [19], [20], [21], [22], [23], [24], [25]] towards a multifaceted mechanism targeting ischaemic stroke damage. While the present work includes the most frequent stroke comorbidity in humans, namely essential hypertension, to better model the human stroke population the results should be confirmed in animals with other stroke comorbidities, in females, and in old animals. In addition, the effects of stroke, hypertension and UA treatment on angiogenic growth should be confirmed by measuring endogenous brain angiogenesis. Based on the present findings, we suggest that activation of the KLF2 pathway is a promising target in acute ischaemic stroke therapy.

Declarations of interest

A.C. is inventor of the patent “Pharmaceutical composition for neuroprotective treatment in patients with ictus comprising citicoline and uric acid”. The other authors declare no competing interests.

Acknowledgements

We are grateful to Belén Pérez and Eva García for helpful technical assistance. This work was supported by Ministerio de Ciencia e Innovación [SAF2014-56111-R]; Generalitat de Catalunya [2017-SGR-645]; Instituto Carlos III [FIS PI13/0091, RIC RD12/0042/0006]; and Instituto de Salud Carlos III (Spain) co-funded by EU FEDER

funds Redes Temáticas de Investigación Cooperativa Sanitaria RETICS-INVICTUS-RD16/019.

References

1. Thomsen MS, Routhe LJ, Moos T. The vascular basement membrane in the healthy and pathological brain. *J Cereb Blood Flow Metab*. 2017;37(10):3300-3317.
2. Thored P, Wood J, Arvidsson A, Cammenga J, Kokaia Z, Lindvall O. Long-term neuroblast migration along blood vessels in an area with transient angiogenesis and increased vascularization after stroke. *Stroke*. 2007;38(11):3032-3039.
3. Ergul A, Alhusban A, Fagan SC. Angiogenesis: a harmonized target for recovery after stroke. *Stroke*. 2012;43(8):2270-2274.
4. Geiseler SJ, Morland C. The Janus Face of VEGF in Stroke. *Int J Mol Sci*. 2018;19(5).
5. Feigin VL, Forouzanfar MH, Krishnamurthi R, Mensah GA, Connor M, Bennett DA, et al. Global and regional burden of stroke during 1990–2010: findings from the Global Burden of Disease Study 2010. *Lancet*. 2014;383(9913):245-255.
6. O'Donnell MJ, Chin SL, Rangarajan S, Xavier D, Liu L, Zhang H, et al. Global and regional effects of potentially modifiable risk factors associated with acute stroke in 32 countries (INTERSTROKE): a case-control study. *Lancet*. 2016;388(10046):761-775.
7. Navaratna D, Guo S, Arai K, Lo EH. Mechanisms and targets for angiogenic therapy after stroke. *Cell Adhesion & Migration*. 2014;3(2):216-223.
8. Powers WJ, Rabinstein AA, Ackerson T, Adeoye OM, Bambakidis NC, Becker K, et al. Guidelines for the Early Management of Patients With Acute Ischemic Stroke: A Guideline for Healthcare Professionals From the

American Heart Association/American Stroke Association. *Stroke*. 2018;49(3):e46-e110.

9. Issa R, Krupinski J, Bujny T, Kumar S, Kaluza J, Kumar P. Vascular endothelial growth factor and its receptor, KDR, in human brain tissue after ischemic stroke. *Lab Invest*. 1999; 79(4):417-425.

10. Zan L, Zhang X, Xi Y, Wu H, Song Y, Teng G, et al. Src regulates angiogenic factors and vascular permeability after focal cerebral ischemia-reperfusion. *Neuroscience*. 2014;262:118-128.

11. Zhang ZG, Zhang L, Tsang W, Soltanian-Zadeh H, Morris D, Zhang R, et al. Correlation of VEGF and angiopoietin expression with disruption of blood-brain barrier and angiogenesis after focal cerebral ischemia. *J Cereb Blood Flow Metab*. 2002;22(4):379-392.

12. Stowe AM, Plautz EJ, Nguyen P, Frost SB, Eisner-Janowicz I, Barbay S, et al. Neuronal HIF-1 alpha protein and VEGFR-2 immunoreactivity in functionally related motor areas following a focal M1 infarct. *J Cereb Blood Flow Metab*. 2008;28(3):612-620.

13. van Bruggen N, Thibodeaux H, Palmer JT, Lee WP, Fu L, Cairns B, et al. VEGF antagonism reduces edema formation and tissue damage after ischemia/reperfusion injury in the mouse brain. *J Clin Invest*. 1999;104(11):1613-1620.

14. Zhang ZG, Zhang L, Jiang Q, Zhang R, Davies K, Powers C, et al. VEGF enhances angiogenesis and promotes blood-brain barrier leakage in the ischemic brain. *J Clin Invest*. 2000;106(7):829-838.

15. Manoonkitiwongsa PS, Schultz RL, McCreery DB, Whitter EF, Lyden PD. Neuroprotection of ischemic brain by vascular endothelial growth factor is

critically dependent on proper dosage and may be compromised by angiogenesis. *J Cereb Blood Flow Metab*. 2004;24(6):693-702.

16. Kimura R, Nakase H, Tamaki R, Sakaki T. Vascular endothelial growth factor antagonist reduces brain edema formation and venous infarction. *Stroke*. 2005;36(6):1259-1263.
17. Zhang HT, Zhang P, Gao Y, Li CL, Wang HJ, Chen LC, et al. Early VEGF inhibition attenuates blood-brain barrier disruption in ischemic rat brains by regulating the expression of MMPs. *Mol Med Rep*. 2017;15(1):57-64.
18. Yu ZF, Bruce-Keller AJ, Goodman Y, Mattson MP. Uric acid protects neurons against excitotoxic and metabolic insults in cell culture, and against focal ischemic brain injury in vivo. *J Neurosci Res*. 1998;53(5):613-625.
19. Romanos E, Planas AM, Amaro S, Chamorro A. Uric acid reduces brain damage and improves the benefits of rt-PA in a rat model of thromboembolic stroke. *J Cereb Blood Flow Metab*. 2007;27(1):14-20.
20. Ma YH, Su N, Chao XD, Zhang YQ, Zhang L, Han F, et al. Thioredoxin-1 attenuates post-ischemic neuronal apoptosis via reducing oxidative/nitrative stress. *Neurochem Int*. 2012;60(5):475-483.
21. Onetti Y, Dantas AP, Perez B, Cugota R, Chamorro A, Planas AM, et al. Middle cerebral artery remodeling following transient brain ischemia is linked to early postischemic hyperemia: a target of uric acid treatment. *Am J Physiol Heart Circ Physiol*. 2015;308(8):H862-874.
22. Justicia C, Salas-Perdomo A, Perez-de-Puig I, Deddens LH, van Tilborg GAF, Castellví C, et al. Uric Acid Is Protective After Cerebral Ischemia/Reperfusion in Hyperglycemic Mice. *Transl Stroke Res*. 2017;8(3):294-305.

23. Dhanesha N, Vazquez-Rosa E, Cintron-Perez CJ, Thedens D, Kort AJ, Chuong V, et al. Treatment with Uric Acid Reduces Infarct and Improves Neurologic Function in Female Mice After Transient Cerebral Ischemia. *J Stroke Cerebrovasc Dis*. 2018;27(5):1412-1416.

24. Aliena-Valero A, Lopez-Morales MA, Burguete MC, Castelló-Ruiz M, Jover-Mengual T, Hervás D, et al. Emergent Uric Acid Treatment is Synergistic with Mechanical Recanalization in Improving Stroke Outcomes in Male and Female Rats. *Neuroscience*. 2018;388:263-273.

25. Jimenez-Xarrie E, Perez B, Dantas AP, Puertas-Umbert L, Martí-Fabregas J, Chamorro Á, et al. Uric Acid Treatment After Stroke Prevents Long-Term Middle Cerebral Artery Remodelling and Attenuates Brain Damage in Spontaneously Hypertensive Rats. *Transl Stroke Res*. 2018. doi:10.1007/s12975-018-0661-8.

26. Chamorro Á, Amaro S, Castellanos M, Segura T, Arenillas J, Martí-Fábregas J, et al. Safety and efficacy of uric acid in patients with acute stroke (URICO-ICTUS): a randomised, double-blind phase 2b/3 trial. *Lancet Neurol*. 2014;13(5):453-460.

27. Llull L, Laredo C, Renu A, Pérez B, Vila E, Obach V, et al. Uric Acid Therapy Improves Clinical Outcome in Women With Acute Ischemic Stroke. *Stroke*. 2015;46(8):2162-2167.

28. Amaro S, Llull L, Renu A, Laredo C, Perez B, Vila E, et al. Uric acid improves glucose-driven oxidative stress in human ischemic stroke. *Ann Neurol*. 2015;77(5):775-783.

29. Amaro S, Laredo C, Renu A, Llull L, Rudilosso S, Obach V, et al. Uric Acid Therapy Prevents Early Ischemic Stroke Progression: A Tertiary Analysis of

the URICO-ICTUS Trial (Efficacy Study of Combined Treatment With Uric Acid and r-tPA in Acute Ischemic Stroke). *Stroke*. 2016;47(11):2874-2876.

30. Chamorro A, Amaro S, Castellanos M, Gomis M, Urra X, Blasco J, et al. Uric acid therapy improves the outcomes of stroke patients treated with intravenous tissue plasminogen activator and mechanical thrombectomy. *Int J Stroke*. 2017;12(4):377-382.
31. Chamorro Á, Dirnagl U, Urra X, Planas AM. Neuroprotection in acute stroke: targeting excitotoxicity, oxidative and nitrosative stress, and inflammation. *Lancet Neurol*. 2016;15(8):869-881.
32. Yu S, Hong Q, Wang Y, Hou K, Wang L, Zhang Y, et al. High concentrations of uric acid inhibit angiogenesis via regulation of the Kruppel-like factor 2-vascular endothelial growth factor-A axis by miR-92a. *Circ J*. 2015;79(11):2487-2498.
33. McConnell BB, Yang VW. Mammalian Kruppel-like factors in health and diseases. *Physiol Rev*. 2010;90(4):1337-1381.
34. Dekker RJ, van Soest S, Fontijn RD, Salamanca S, de Groot PG, VanBavel E, et al. Prolonged fluid shear stress induces a distinct set of endothelial cell genes, most specifically lung Kruppel-like factor (KLF2). *Blood*. 2002;100(5):1689-1698.
35. Dekker RJ, van Thienen JV, Rohlena J, de Jager SC, Elderkamp YW, Seppen J, et al. Endothelial KLF2 Links Local Arterial Shear Stress Levels to the Expression of Vascular Tone-Regulating Genes. *Am J Pathol*. 2005;167(2):609-618.

36. Sen-Banerjee S, Mir S, Lin Z, Hamik A, Atkins GB, Das H, et al. Kruppel-like factor 2 as a novel mediator of statin effects in endothelial cells. *Circulation*. 2005;112(5):720-726.

37. Parmar KM, Larman HB, Dai G, Zhang Y, Wang ET, Moorthy SN, et al. Integration of flow-dependent endothelial phenotypes by Kruppel-like factor 2. *J Clin Invest*. 2006;116(1):49-58.

38. Young A, Wu W, Sun W, Benjamin Larman H, Wang N, Li YS, et al. Flow activation of AMP-activated protein kinase in vascular endothelium leads to Kruppel-like factor 2 expression. *Arterioscler Thromb Vasc Biol*. 2009;29(11):1902-1908.

39. Komaravolu RK, Adam C, Moonen JR, Harmsen MC, Goebeler M, Schmidt M. Erk5 inhibits endothelial migration via KLF2-dependent down-regulation of PAK1. *Cardiovasc Res*. 2015;105(1):86-95.

40. Nayak L, Shi H, Atkins GB, Lin Z, Schmaier AH, Jain MK. The thromboprotective effect of bortezomib is dependent on the transcription factor Kruppel-like factor 2 (KLF2). *Blood*. 2014;123(24):3828-3831.

41. Shi H, Sheng B, Zhang F, Wu C, Zhang R, Zhu J, et al. Kruppel-like factor 2 protects against ischemic stroke by regulating endothelial blood brain barrier function. *Am J Physiol Heart Circ Physiol*. 2013;304(6):H796-805.

42. Justicia, C, Martín, A, Rojas, S, Gironella, M, Cervera, A, Panés, J, et al. Anti-VCAM-1 antibodies did not protect against ischemic damage neither in rats nor in mice. *J Cereb Blood Flow Metab*. 2006;26(3):321–332.

43. Perez-Asensio FJ, de la Rosa X, Jimenez-Altayo F, Gorina R, Martínez E, Messeguer A, et al. Antioxidant CR-6 protects against reperfusion injury after

a transient episode of focal brain ischemia in rats. *J Cereb Blood Flow Metab*. 2010;30(3):638-652.

44. Pedragosa J, Salas-Perdomo A, Gallizioli M, Cugota R, Miró-Mur F, Briansó F, et al. CNS-border associated macrophages respond to acute ischemic stroke attracting granulocytes and promoting vascular leakage. *Acta Neuropathol Commun*. 2018;6(1):76.

45. Weksler BB, Subileau EA, Perriere N, Charneau P, Holloway K, Leveque M, et al. Blood-brain barrier-specific properties of a human adult brain endothelial cell line. *FASEB J*. 2005;19(13):1872-1874.

46. Weksler B, Romero IA, Couraud PO. The hCMEC/D3 cell line as a model of the human blood brain barrier. *Fluids Barriers CNS*. 2013;10(1):16.

47. Sun P, Esteban G, Inokuchi T, Marco-Contelles J, Weksler BB, Romero IA, et al. Protective effect of the multitarget compound DPH-4 on human SSAO/VAP-1-expressing hCMEC/D3 cells under oxygen-glucose deprivation conditions: an in vitro experimental model of cerebral ischaemia. *Br J Pharmacol*. 2015;172(22):5390-5402.

48. Deng X, Yang Q, Kwiatkowski N, Sim T, McDermott U, Settleman JE, et al. Discovery of a benzo[e]pyrimido-[5,4-b][1,4]diazepin-6(11H)-one as a Potent and Selective Inhibitor of Big MAP Kinase 1. *ACS Med Chem Lett*. 2011;2(3):195-200.

49. Sun P, Hernandez-Guillamon M, Campos-Martorell M, Simats A, Montaner J, Unzeta M, et al. Simvastatin blocks soluble SSAO/VAP-1 release in experimental models of cerebral ischemia: Possible benefits for stroke-induced inflammation control. *Biochim Biophys Acta Mol Basis Dis*. 2018;1864(2):542-553.

50. Vicente D, Hernandez B, Segura V, Pascual D, Fornaciari G, Monto F, et al. Methodological Approach to Use Fresh and Cryopreserved Vessels as Tools to Analyze Pharmacological Modulation of the Angiogenic Growth. *J Cardiovasc Pharmacol*. 2016;68(3):230-240.

51. Marrone G, Russo L, Rosado E, Hide D, García-Cardeña G, García-Pagán JC, et al. The transcription factor KLF2 mediates hepatic endothelial protection and paracrine endothelial-stellate cell deactivation induced by statins. *J Hepatol*. 2013;58(1):98-103.

52. Xu Y, Xu S, Liu P, Koroleva M, Zhang S, Si S, et al. Suberanilohydroxamic Acid as a Pharmacological Kruppel-Like Factor 2 Activator That Represses Vascular Inflammation and Atherosclerosis. *J Am Heart Assoc*. 2017;6(12).

53. Novensa L, Selent J, Pastor M, Sandberg K, Heras M, Dantas AP. Equine estrogens impair nitric oxide production and endothelial nitric oxide synthase transcription in human endothelial cells compared with the natural 17{beta}-estradiol. *Hypertension*. 2010;56(3):405-411.

54. Bhattacharya R, Senbanerjee S, Lin Z, Mir S, Hamik A, Wang P, et al. Inhibition of vascular permeability factor/vascular endothelial growth factor-mediated angiogenesis by the Kruppel-like factor KLF2. *J Biol Chem*. 2005;280(32):28848-28851.

55. Lin Z, Natesan V, Shi H, Dong F, Kawanami D, Mahabeleshwar GH, et al. Kruppel-like factor 2 regulates endothelial barrier function. *Arterioscler Thromb Vasc Biol*. 2010;30(10):1952-1959.

56. Slevin M, Krupinski J, Slowik A, Kumar P, Szczudlik A, Gaffney J. Serial Measurement of Vascular Endothelial Growth Factor and Transforming

Growth Factor-β1 in Serum of Patients With Acute Ischemic Stroke. *Stroke*. 2000;31(8):1863-1870.

57. Lee SC, Lee KY, Kim YJ, Kim SH, Koh SH, Lee YJ. Serum VEGF levels in acute ischaemic strokes are correlated with long-term prognosis. *Eur J Neurol.* 2010;17(1):45-51.

58. Matsuo R, Ago T, Kamouchi M, Kuroda J, Kuwashiro T, Hata J, et al. Clinical significance of plasma VEGF value in ischemic stroke - research for biomarkers in ischemic stroke (REBIOS) study. *BMC Neurol*. 2013;13:32.

59. Tureyen K, Kapadia R, Bowen KK, Satriotomo I, Liang J, Feinstein DL, et al. Peroxisome proliferator-activated receptor-gamma agonists induce neuroprotection following transient focal ischemia in normotensive, normoglycemic as well as hypertensive and type-2 diabetic rodents. *J Neurochem*. 2007;101(1):41-56.

60. Yin KJ, Hamblin M, Fan Y, Zhang J, Chen YE. Krupple-like factors in the central nervous system: novel mediators in stroke. *Metab Brain Dis*. 2015;30(2):401-410.

61. Fan Y, Lu H, Liang W, Hu W, Zhang J, Chen YE. Kruppel-like factors and vascular wall homeostasis. *J Mol Cell Biol*. 2017;9(5):352-363.

62. Yang M, Aragon M, Murfee WL. Angiogenesis in mesenteric microvascular networks from spontaneously hypertensive versus normotensive rats. *Microcirculation*. 2011;18(7):574-582.

63. Sun Y, Jin K, Xie L, Childs J, Mao XO, Logvinova A, et al. VEGF-induced neuroprotection, neurogenesis, and angiogenesis after focal cerebral ischemia. *J Clin Invest*. 2003;111(12):1843-1851.

64. Krupinski J, Kaluza J, Kumar P, Kumar S, Wang JM, Role of angiogenesis in patients with cerebral ischemia stroke, *Stroke*. 1994; 25(9):1794-1798.

65. Krueger M, Bechmann I, Immig K, Reichenbach A, Hartig W, Michalski D. Blood-brain barrier breakdown involves four distinct stages of vascular damage in various models of experimental focal cerebral ischemia. *J Cereb Blood Flow Metab*. 2015;35(2):292-303.

66. Endres M, Laufs U, Huang Z, Nakamura T, Huang P, Moskowitz MA, et al. Stroke protection by 3-hydroxy-3-methylglutaryl (HMG)-CoA reductase inhibitors mediated by endothelial nitric oxide synthase. *Proc Natl Acad Sci U S A*. 1998;95(15):8880-8885.

67. Sukumari-Ramesh S, Alleyne CH, Jr., Dhandapani KM. The Histone Deacetylase Inhibitor Suberoylanilide Hydroxamic Acid (SAHA) Confers Acute Neuroprotection After Intracerebral Hemorrhage in Mice. *Transl Stroke Res*. 2016;7(2):141-148.

68. Tang Y, Lin YH, Ni HY, Dong J, Yuan HJ, Zhang Y, et al. Inhibiting Histone Deacetylase 2 (HDAC2) Promotes Functional Recovery From Stroke. *J Am Heart Assoc*. 2017;6(10).

69. Kawanami D, Mahabeleshwar GH, Lin Z, Atkins GB, Hamik A, Haldar SM, et al. Kruppel-like factor 2 inhibits hypoxia-inducible factor 1alpha expression and function in the endothelium. *J Biol Chem*. 2009;284(31):20522-20530.

70. Bartoszewski R, Serocki M, Janaszak-Jasiecka A, Bartoszewska S, Kochan-Jamrozy K, Piotrowski A, et al. miR-200b downregulates Kruppel Like Factor 2 (KLF2) during acute hypoxia in human endothelial cells. *Eur J Cell Biol*. 2017;96(8):758-766.

71. Liu Y, Huang Y, Xu Y, Qu P, Wang M. Memantine protects against ischemia/reperfusion-induced brain endothelial permeability. *IUBMB Life*. 2018;70(4):336-343.

72. Krueger M, Hartig W, Reichenbach A, Bechmann I, Michalski D. Blood-brain barrier breakdown after embolic stroke in rats occurs without ultrastructural evidence for disrupting tight junctions. *PLoS One*. 2013;8(2):e56419.

73. Reeson P, Tennant KA, Gerrow K, Wang J, Weiser Novak S, Thompson K, et al. Delayed inhibition of VEGF signaling after stroke attenuates blood-brain barrier breakdown and improves functional recovery in a comorbidity-dependent manner. *J Neurosci*. 2015;35(13):5128-5143.

74. De Bock M, Culot M, Wang N, Bol M, Decrock E, De Vuyst E, et al. Connexin channels provide a target to manipulate brain endothelial calcium dynamics and blood-brain barrier permeability. *J Cereb Blood Flow Metab*. 2011;31(9):1942-1957.

75. Lin WY, Chang YC, Ho CJ, Huang CC. Ischemic preconditioning reduces neurovascular damage after hypoxia-ischemia via the cellular inhibitor of apoptosis 1 in neonatal brain. *Stroke*. 2013;44(1):162-169.

Figure Legends

Fig. 1. Effect of uric acid on brain damage after cerebral ischaemia (90 min)/reperfusion (24 h) (I/R) in WKY and SHR rats. (A) WKY and SHR rats were treated (i.v.) with uric acid (16 mg/kg) or vehicle (Locke's buffer) at 120 min after ischaemia (i.e. 30 min after reperfusion onset). After 24 h of reperfusion, rats were euthanized, the brain was removed and infarct volume was assessed in 2-mm-thick coronal sections stained with 2,3,5-triphenyltetrazolium chloride (TTC). MCAo, middle cerebral artery occlusion. (B) and (C) Representative images of TTC-stained coronal brain sections and analysis of total, cortical and subcortical infarct volumes in WKY and SHR rats, respectively. (D) Analysis of neurological score in WKY and SHR rats. Results are mean ± SEM from WKY (vehicle: n = 6; uric acid: n = 6) and SHR (vehicle: n = 6; uric acid: n = 6) rats. $^{\#}P < 0.05$, $^{\#\#}P < 0.01$ vs. WKY I/R + vehicle; $^{**}P < 0.01$ vs. vehicle by Mann-Whitney.

Fig. 2. Effect of uric acid on *in vivo* BBB integrity. (A) WKY and SHR rats were subjected to ischaemia (90 min)/reperfusion (24 h) (I/R) and treated (i.v.) with uric acid (16 mg/kg) or vehicle (Locke's buffer). Animals received (i.v.) Evans blue (2% in saline; 80 mg/kg of body weight) at 22 h of reperfusion, and two hours later, the animals were perfused through the heart with saline. MCAo, middle cerebral artery occlusion. (B) Representative images of coronal brain sections showing Evans blue extravasation and analysis (bottom) of Evans blue volume in WKY and SHR rats. Results are mean ± SEM from WKY (vehicle: n = 5; uric acid: n = 4) and SHR (vehicle: n = 7; uric acid: n = 4) rats. $^{\#\#}P < 0.01$ vs. WKY I/R + vehicle; $^{*}P < 0.05$ vs. vehicle by Mann-Whitney.

Fig. 3. Influence of hypertension and uric acid treatment on the MCA angiogenic response after cerebral ischaemia (90 min)/reperfusion (24 h) (I/R). (A) WKY and SHR rats were treated (i.v.) with uric acid (16 mg/kg) or vehicle (Locke's buffer) at 120 min after ischaemia (i.e. 30 min after reperfusion onset). After 24 h of reperfusion, rats were euthanized and the ipsilateral (ischaemic) MCA was dissected and cultured in Matrigel for the analysis of angiogenic growth at day 4, 5, 6, 7, 10 and 14 after seeding. MCAo, middle cerebral artery occlusion. (B) Representative images of neovessel sprouting at day 5 in ipsilateral MCA from sham and ischaemic WKY and SHR rats. Red dotted lines represent the length of the longest vessel sprouting from the outer surface of the MCA (starting point). (C) Analysis of neovessel growth progression in ipsilateral MCA from vehicle-treated sham and ischaemic WKY and SHR rats. (D) and (E) Comparison of neovessel growth progression in ipsilateral MCA from uric acid- and vehicle-treated ischaemic WKY and SHR rats, respectively. NS, not significant. Results are mean ± SEM from WKY (sham + vehicle: n = 5; I/R + vehicle: n = 6; I/R + uric acid: n = 6) and SHR (sham + vehicle: n = 6; I/R + vehicle: n = 6; I/R + uric acid: n = 6) rats. $^{++}P < 0.01$ SHR I/R + vehicle vs. SHR sham + vehicle; $^{\#}P < 0.05$ SHR I/R + vehicle vs. WKY I/R + vehicle; $^{*}P < 0.05$ SHR I/R + vehicle vs. SHR I/R + uric acid by two-way ANOVA.

Fig. 4. Influence of hypertension and uric acid treatment on circulating VEGF-A levels after ischaemic stroke. (A) Plasma levels of VEGF-A in WKY and SHR rats subjected to cerebral ischaemia (90 min)/reperfusion (24 h) (I/R) and treated (i.v.) with uric acid (16 mg/kg) or vehicle (Locke's buffer) at 120 min after ischaemia (i.e. 30 min after reperfusion onset). VEGF-A levels in vehicle-treated sham-operated WKY and SHR rats are also shown. Results are mean ± SEM from WKY (sham: n = 13; vehicle: n = 11; uric acid: n = 11) and SHR (sham: n = 17; vehicle: n = 11; uric acid: n = 11) rats.

$^{+}P < 0.05$ vs. sham + vehicle by Kruskal-Wallis. (B) Serum VEGF-A levels in normotensive and hypertensive acute ischaemic stroke patients before (T_0) and 6 to 12 h after (T_1) treatment with placebo or uric acid (UA). Box-whisker plots (box, 25% to 75% interquartile range [IQR]; central horizontal bar, median; outer horizontal bars, 10% to 90% IQR) represent the concentration values from normotensive (placebo: n = 7; UA: n = 13) and hypertensive (placebo: n = 22; UA: n = 14) patients. $^{*}P < 0.05$ UA vs. placebo by Mann-Whitney.

Fig. 5. Influence of hypertension and uric acid treatment on mRNA levels of VEGF-A, VEGFR2, and KLF2 in cerebral arteries from WKY and SHR rats subjected to cerebral ischaemia (90 min)/reperfusion (24 h) (I/R). mRNA levels are expressed as $2^{-\Delta\Delta Ct}$ using GAPDH and 18S as internal controls. Results are mean ± SEM from WKY (n = 2-6 per group) and SHR (n = 3-6 per group) rats. $^{*}P < 0.05$ vs. I/R + vehicle by Kruskal-Wallis test.

Fig. 6. Effect of uric acid on *in vitro* BBB integrity. (A) Human cerebral microvascular endothelial hCMEC/D3 cells were seeded onto transwell inserts and allowed to grow for 4 days before applying the treatments. Cells were subjected to 16 h of oxygen and glucose deprivation (OGD) followed by 24 h of re-oxygenation in the presence of uric acid (10-1000 µM) or UA (50 µM) + XMD8-92 (1-30 µM), and the permeability was assessed by measuring fluorescein isothiocyanate dextran passage. (B) Effect of OGD + re-oxygenation and uric acid (10-1000 µM) incubation on permeability to dextran in endothelial hCMEC/D3 cells. Results are mean ± SEM from n = 6 independent experiments. $^{+++}P < 0.001$, $^{+}P < 0.05$ vs. non-treated cells in normoxia; $^{*}P < 0.05$, $^{**}P < 0.01$ vs. non-treated cells under OGD + re-oxygenation by one-way ANOVA. (C)

Protein expression of tight and adherens junction proteins occludin (60 kDa), zonula occludens-1 (ZO-1; 250 kDa) and claudin-5 (20 kDa); and adherens junction protein VE-cadherin (130 kDa). Beta-actin (42 KDa) was used as loading control. Bar graphs (bottom) show the results of densitometric analyses from pooled data normalised for non-treated cells in normoxia average values. Results are mean ± SEM from n = 4 independent experiments. $^{\#}P < 0.05$ vs. non-treated cells in normoxia by one-way ANOVA. (D) Western blot analysis for KLF2 (40 kDa) protein expression in endothelial hCMEC/D3 cells subjected to OGD + re-oxygenation. Beta-actin (42 KDa) was used as loading control. Bar graphs (bottom) show the results of densitometric analyses from pooled data normalised for non-treated cells in normoxia average values. Results are mean ± SEM from n = 3-4 independent experiments. $^{+}P < 0.05$ vs. non-treated cells in normoxia by one-way ANOVA. (E) Effect of OGD + re-oxygenation and uric acid (50 μM) + XMD8-92 (1-30 μM) incubation on permeability to dextran in endothelial hCMEC/D3 cells. Results are mean ± SEM from n = 3 independent experiments. $^{+++}P < 0.001$ vs. non-treated cells in normoxia; $^{**}P < 0.05$, $^{***}P < 0.001$ vs. non-treated cells under OGD + re-oxygenation by one-way ANOVA.

Fig. 7. Influence of exogenous uric acid incubation on the MCA angiogenic response after cerebral ischaemia/reperfusion (I/R). (A) WKY and SHR rats were subjected to cerebral I (90 min)/R (30 min) and the ipsilateral (ischaemic) MCA was dissected and incubated in growth medium with Matrigel in the presence (23.5 h) of vehicle (Locke's buffer) and uric acid (10-30 μM). Angiogenic growth was analysed at day 4, 5, 6, 7, 10 and 14 after seeding. MCAo, middle cerebral artery occlusion. (B) and (C) Representative images of neovessel sprouting at day 6 and analysis of neovessel growth progression (bottom) in ipsilateral MCA from ischaemic WKY and SHR rats,

respectively, exogenously treated with vehicle or uric acid. Red dotted lines represent the length of the longest vessel sprouting from the outer surface of the MCA (starting point). NS, not significant. Results are mean ± SEM from WKY (n = 5) and SHR (n = 5) rats (n = 5 arteries per group). *P < 0.05 vs. I/R + uric acid 10 or 30 μM by two-way ANOVA.

Fig. 8. Influence of KLF2 on the effects of exogenous uric acid incubation on the MCA angiogenic response after cerebral ischaemia/reperfusion (I/R). WKY and SHR rats were subjected to cerebral I (90 min)/R (30 min) and the ipsilateral (ischaemic) MCA was dissected and incubated in growth medium with Matrigel in the presence (23.5 h) of vehicle (Locke's buffer), uric acid (30 μM), uric acid (30 μM) + XMD8-92 (5 μM), DMSO, simvastatin (10 μM), or SAHA (10 μM). Angiogenic growth was analysed at day 4, 5, 6, 7, 10 and 14 after seeding. KLF2 immunofluorescence was studied in ipsilateral MCA incubated (23.5 h) in culture medium with vehicle or uric acid (30 μM). (A) Representative photomicrographs and quantification of KLF2 immunofluorescence (red) in confocal microscopic sections of ipsilateral MCA from ischaemic SHR rats. Natural autofluorescence of elastin (green) and nuclear staining with Hoechst (blue) are also shown. Arrows indicate localization of representative nuclei with increased KLF2 fluorescence. Results are the mean ± SEM from SHR (n = 6) rats (n = 6 arteries per group). P = 0.065 by Mann-Whitney. (B) and (C) Representative images of neovessel sprouting at day 6 in ipsilateral MCA from ischaemic SHR rats exogenously treated, respectively, with uric acid or uric acid + XMD8-92; and DMSO, simvastatin, or SAHA. Red dotted lines represent the length of the longest vessel sprouting from the outer surface of the MCA (starting point). NS, not significant. Results are mean ±

SEM from SHR (n = 7) rats (n = 6-7 arteries per group). *P < 0.05 vs. I/R + uric acid 30 μM; ^{+}P < 0.05, ^{++}P < 0.01 vs. I/R + DMSO by two-way ANOVA.

Table 1. Percentage changes in cortical cerebral blood flow (CBF) during ischaemia (90 min) and reperfusion (first 15 min) with respect to basal values in rats submitted to 24 h of reperfusion.

	WKY		SHR	
% Basal CBF	**Vehicle (11)**	**uric acid (10)**	**vehicle (13)**	**uric acid (10)**
ischaemia	41.6 ± 4.0	39.1 ± 4.7	43.9 ± 3.1	47.1 ± 3.3
reperfusion	89.0 ± 12.5	68.3 ± 4.0	114.1 ± 6.6*	105.9 ± 9.0***

Results are the mean ± SEM from WKY and SHR rats. The number of animals is shown in parenthesis. *$P < 0.05$, ***$P < 0.001$ vs. the same group in WKY rats by Mann-Whitney test.

Table 2. General traits of the included URICO-ICTUS population according to hypertension history and treatment allocation (uric acid vs. placebo).

	No Hypertensives (n = 20)		**Hypertensives (n = 36)**	
Treatment allocation	**placebo**	**uric acid**	**placebo**	**uric acid**
	n = 7	**n = 13**	**n = 22**	**n = 14**
Age (years), median (IQR)	81 (78-89)	76 (63-80)*	80 (74-84)	79 (64-83)
Sex (males), %	14	31	46	64
Smoking habit, %	0	15	5	7
Diabetes, %	14	23	36	23
Dyslipidemia, %	14	15	27	64*
Atrial Fibrillation, %	29	8	18	24
Mean Blood Pressure (mmHg), mean (SD)	98 (96-120)	100 (91-115)	108 (99-117)	99 (90-108)
Glucose (mg/dl), median (IQR)	140 (119-178)	107 (99-116)*	126 (109-157)	115 (91-143)
Pre-treatment NIHSS score, median (IQR)	16 (9-19)	11 (8-14)	11 (9-18)	16 (11-18)
Mechanical thrombectomy (%)	14	46	31	50
Cardioembolic origin (%) (vs. other)	57	46	54	71
Treatment with statins, n (%)	4 (57)	8 (62)	13 (59)	10 (71)

IQR, interquartile range; SD, standard deviation; NIHSS, National institute of Health Stroke Scale; *$P < 0.05$, placebo vs. uric acid by Mann-Whitney.

Table 3. Percentage changes in cortical cerebral blood flow (CBF) during ischaemia (90 min) and reperfusion (first 15 min) with respect to basal values in rats submitted to 30 min of reperfusion.

% Basal CBF	WKY (5)	SHR (12)
ischaemia	46.4 ± 6.2	46.0 ± 2.6
reperfusion	70.3 ± 2.4	117.8 ± 13.3**

Results are the mean ± SEM from WKY and SHR rats. The number of animals is shown in parenthesis.

***P* < 0.01 vs. WKY rats by Mann-Whitney test.

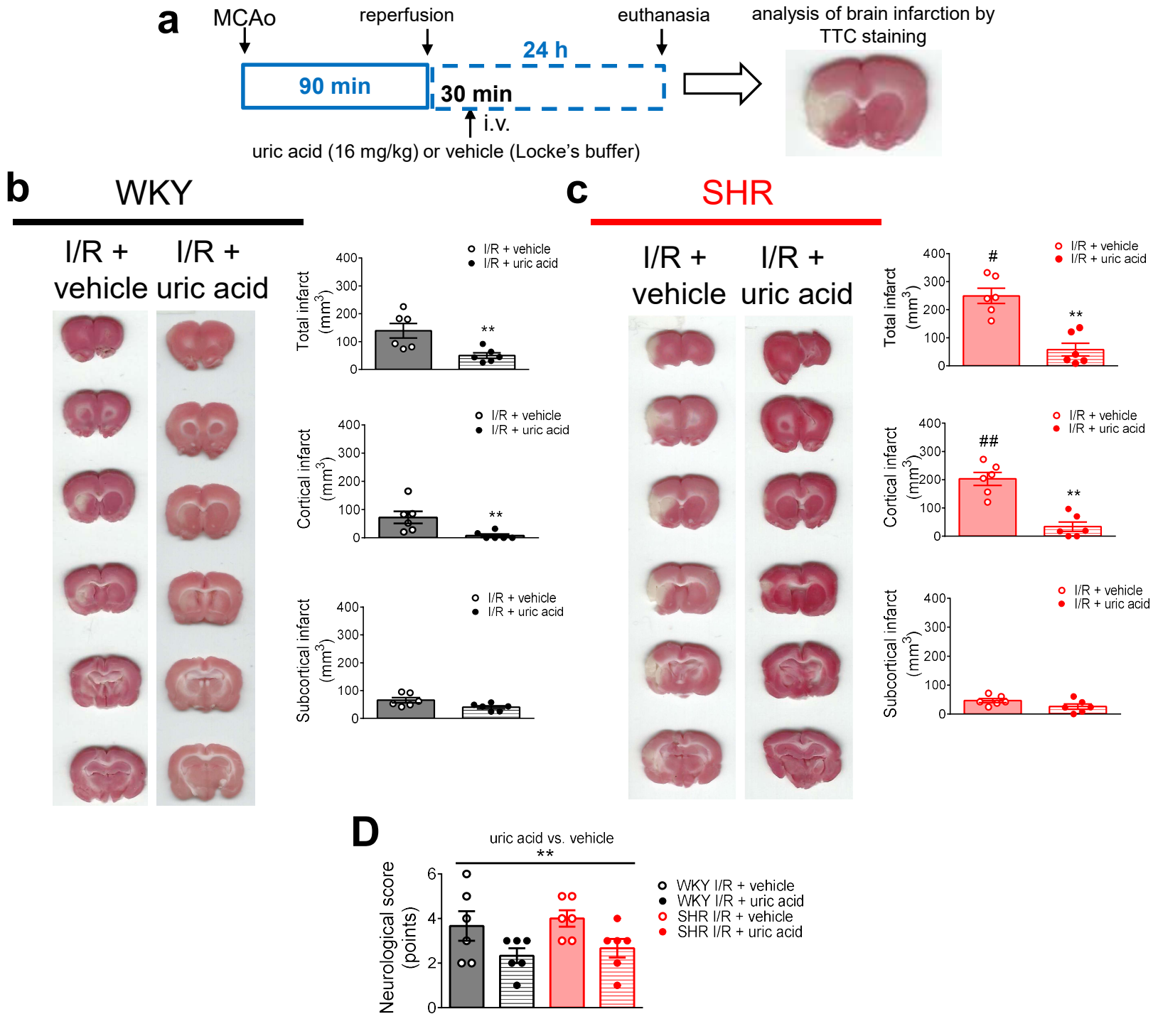
a
MCAo
reperfusion
euthanasia
analysis of brain infarction by TTC staining
24 h
90 min
30 min
i.v.
uric acid (16 mg/kg) or vehicle (Locke's buffer)
b
WKY
I/R + vehicle
I/R + uric acid
Total infarct (mm3)
Cortical infarct (mm3)
Subcortical infarct (mm3)
c
SHR
D
uric acid vs. vehicle
Neurological score (points)
WKY I/R + vehicle
WKY I/R + uric acid
SHR I/R + vehicle
SHR I/R + uric acid

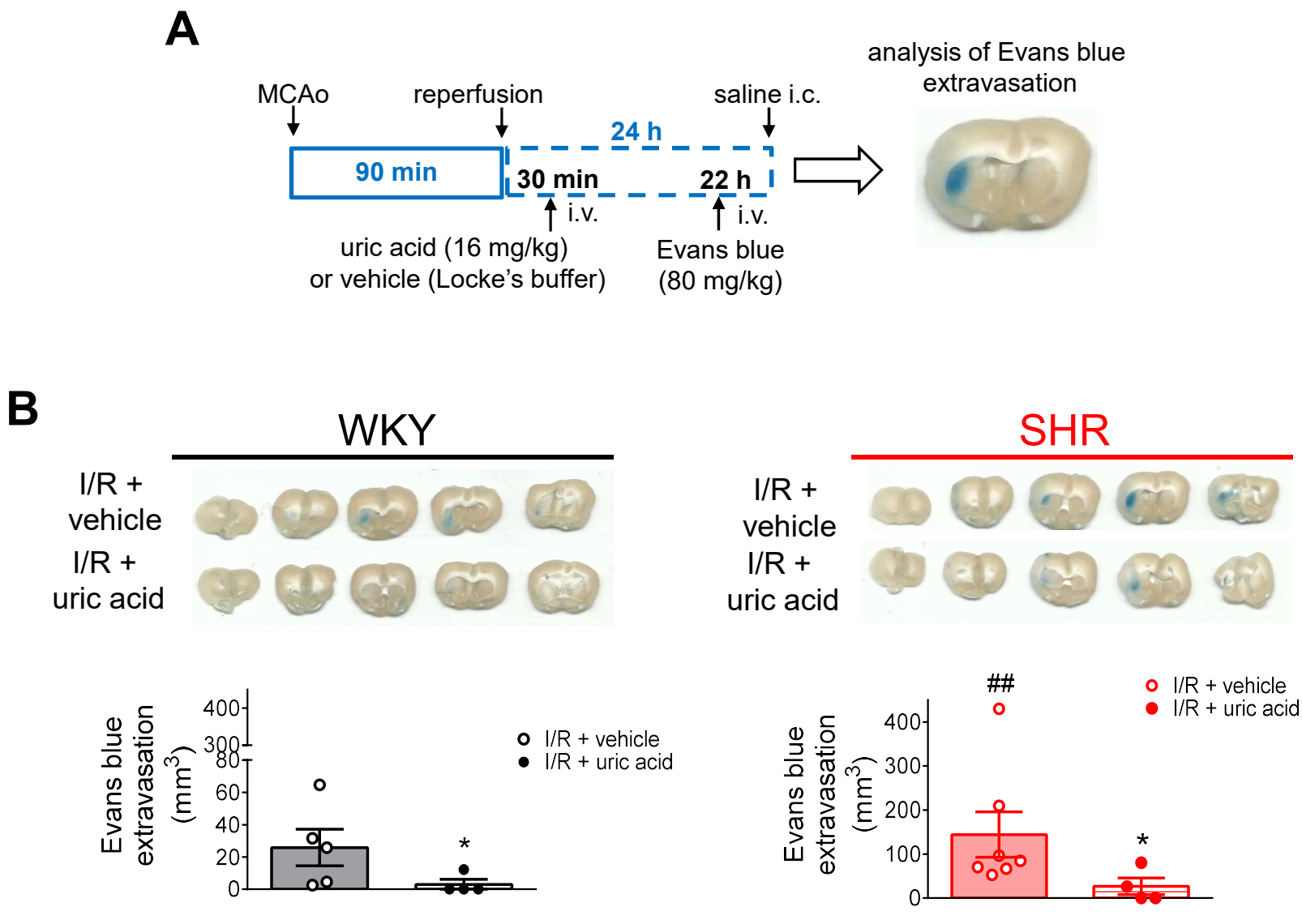
A
MCAo
reperfusion
saline i.c.
24 h
90 min
30 min
22 h
i.v.
i.v.
uric acid (16 mg/kg)
or vehicle (Locke's buffer)
Evans blue
(80 mg/kg)
analysis of Evans blue
extravasation
B
WKY
SHR
I/R +
vehicle
I/R +
uric acid
Evans blue
extravasation
(mm3)
400
300
80
60
40
20
0
I/R + vehicle
I/R + uric acid
*
##
200
100

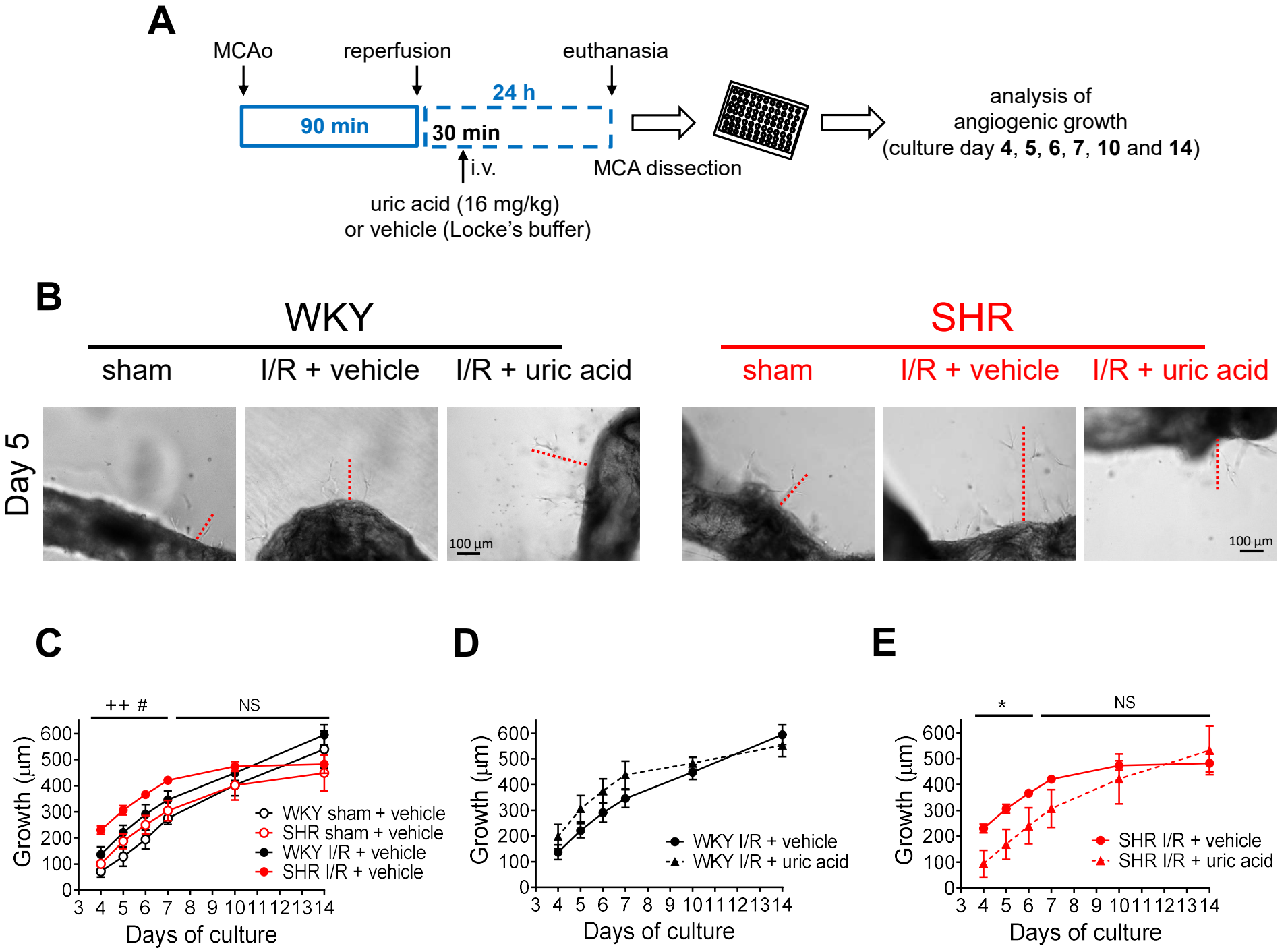
A
MCAo
reperfusion
euthanasia
24 h
90 min
30 min
i.v.
uric acid (16 mg/kg)
or vehicle (Locke's buffer)
MCA dissection
analysis of
angiogenic growth
(culture day 4, 5, 6, 7, 10 and 14)
B
WKY
SHR
sham
I/R + vehicle
I/R + uric acid
sham
I/R + vehicle
I/R + uric acid
Day 5
100 µm
100 µm
C
++ #
NS
Growth (µm)
Days of culture
WKY sham + vehicle
SHR sham + vehicle
WKY I/R + vehicle
SHR I/R + vehicle
D
Growth (µm)
Days of culture
WKY I/R + vehicle
WKY I/R + uric acid
E
*
NS
Growth (µm)
Days of culture
SHR I/R + vehicle
SHR I/R + uric acid

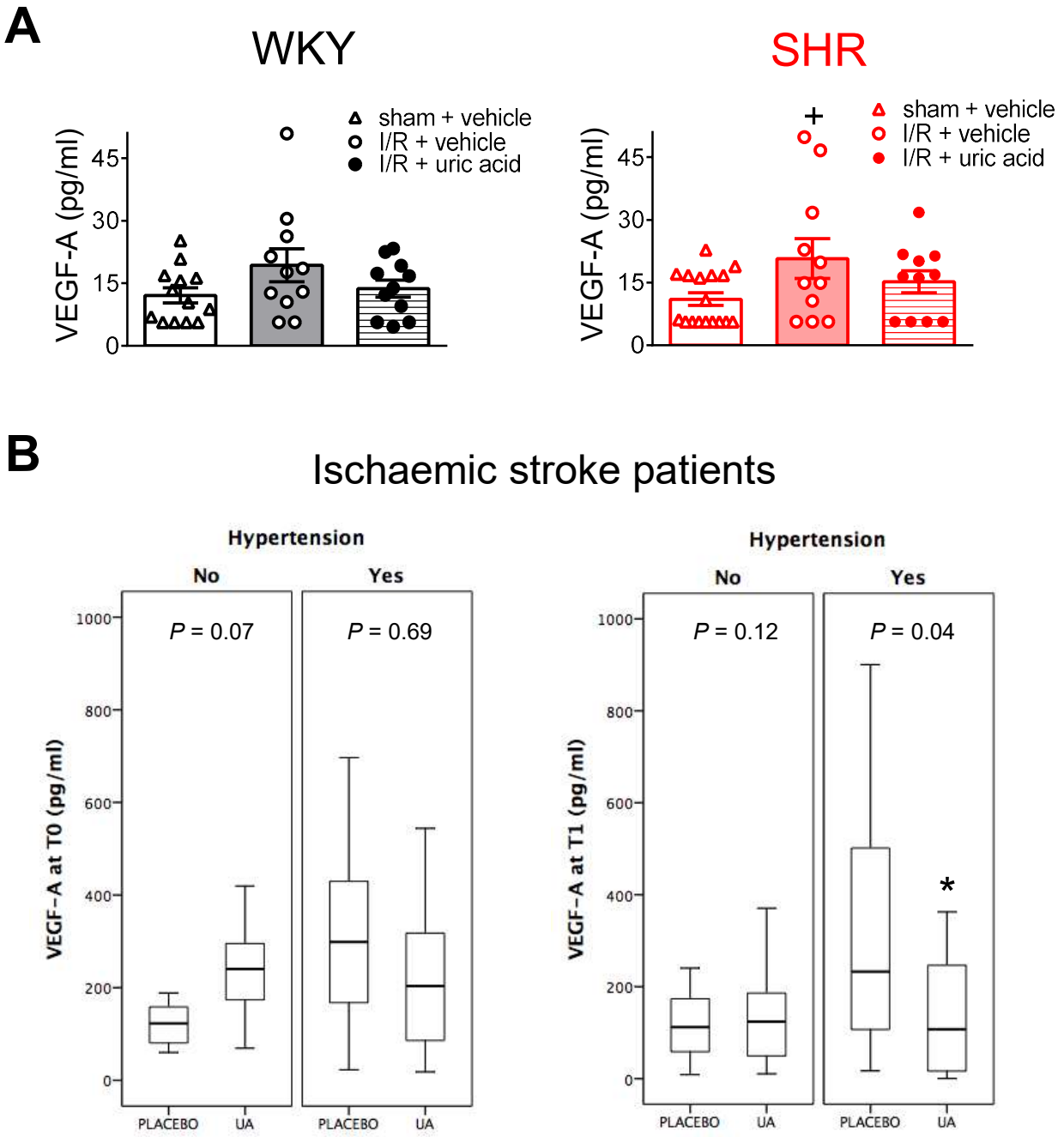
A
WKY
SHR
sham + vehicle
I/R + vehicle
I/R + uric acid
VEGF-A (pg/ml)
0
15
30
45
B
Ischaemic stroke patients
Hypertension
No
Yes
P = 0.07
P = 0.69
P = 0.12
P = 0.04
VEGF-A at T0 (pg/ml)
VEGF-A at T1 (pg/ml)
0
200
400
600
800
1000
PLACEBO
UA
*

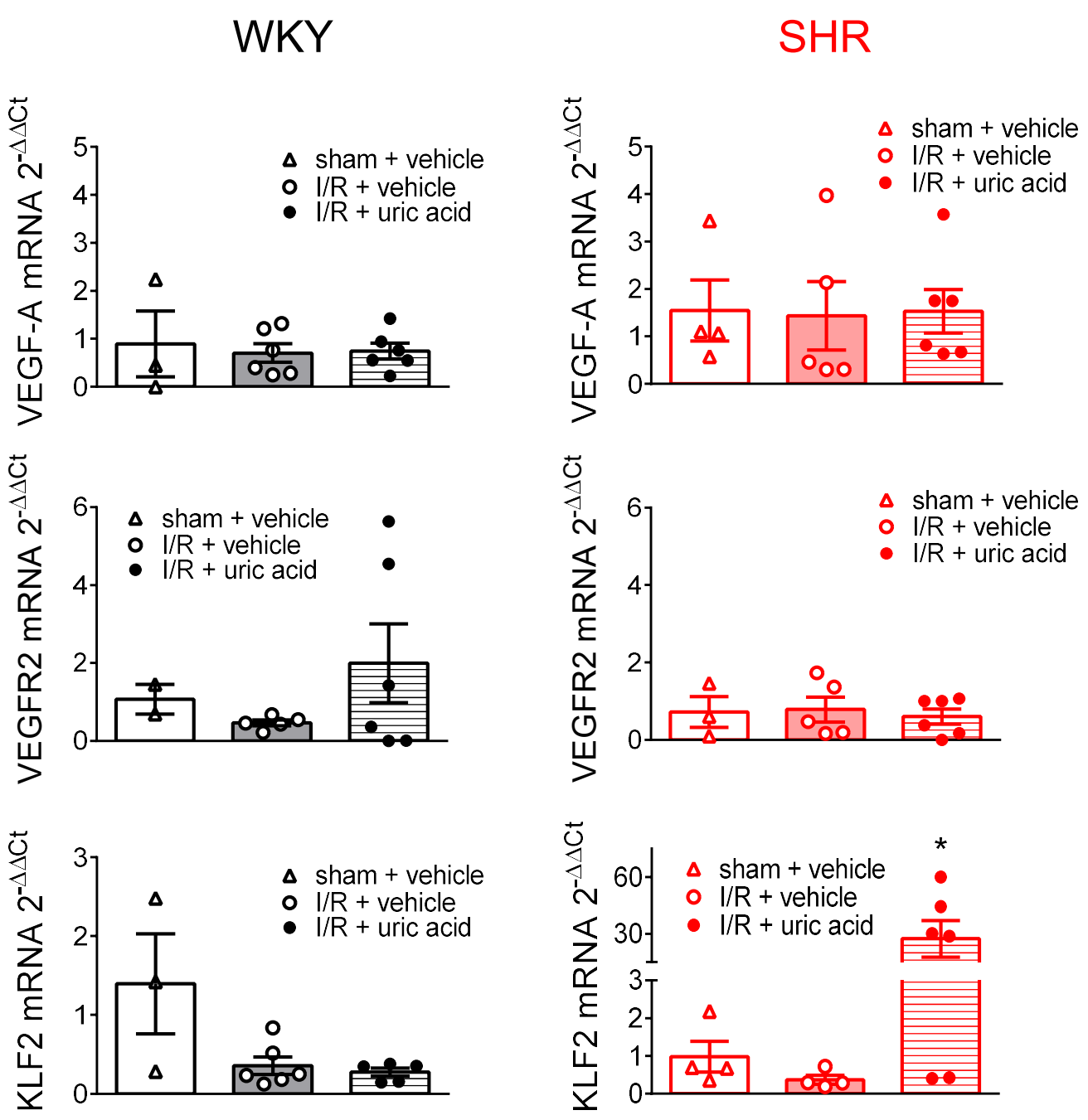
WKY
SHR
VEGF-A mRNA 2-ΔΔCt
VEGFR2 mRNA 2-ΔΔCt
KLF2 mRNA 2-ΔΔCt
sham + vehicle
I/R + vehicle
I/R + uric acid
*

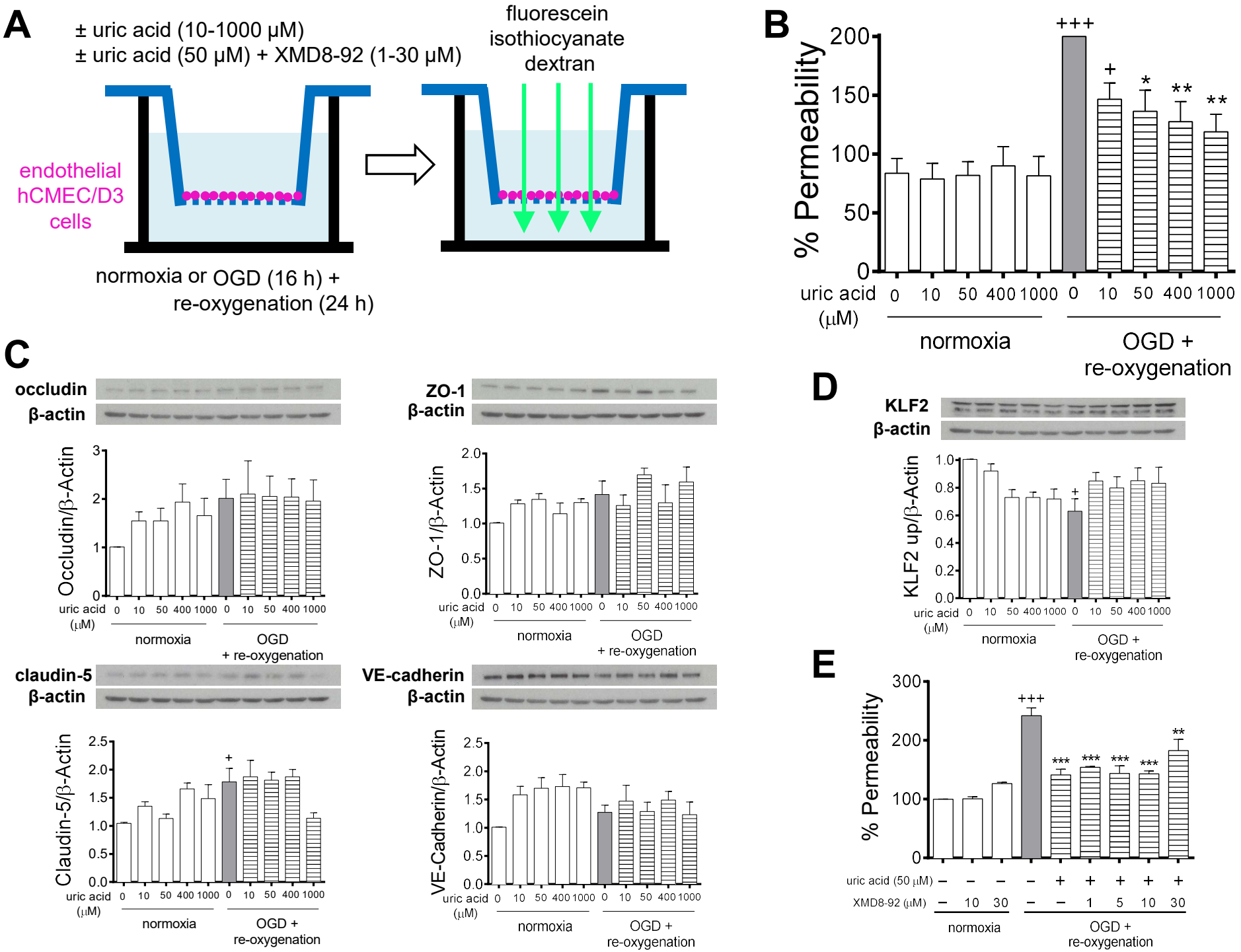
A
± uric acid (10-1000 µM)
± uric acid (50 µM) + XMD8-92 (1-30 µM)
fluorescein isothiocyanate dextran
endothelial hCMEC/D3 cells
normoxia or OGD (16 h) + re-oxygenation (24 h)
B
% Permeability
uric acid (µM)
normoxia
OGD + re-oxygenation
C
occludin
β-actin
Occludin/β-Actin
ZO-1
ZO-1/β-Actin
claudin-5
Claudin-5/β-Actin
VE-cadherin
VE-Cadherin/β-Actin
D
KLF2
KLF2 up/β-Actin
E
XMD8-92 (µM)

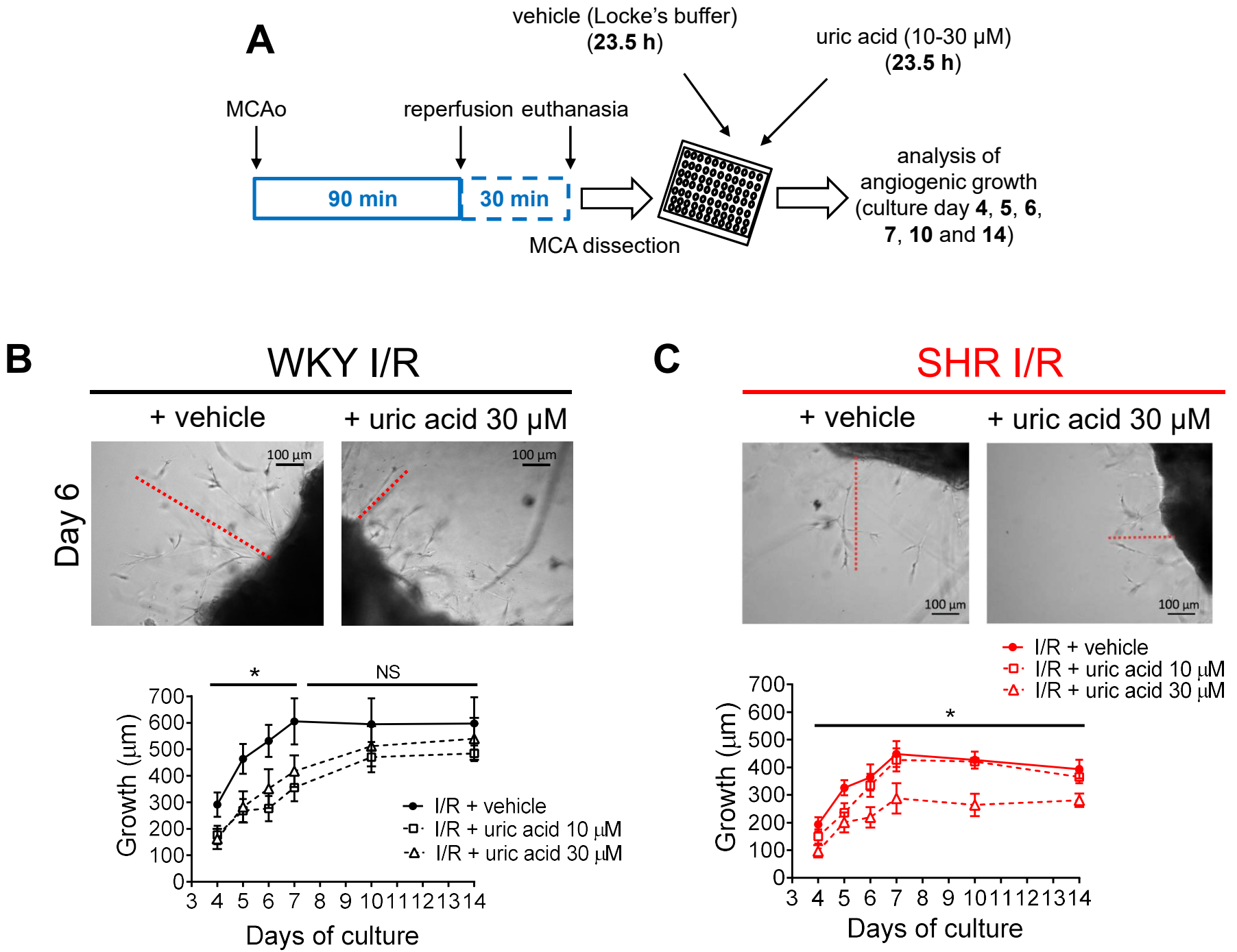
A
vehicle (Locke's buffer)
(23.5 h)
uric acid (10-30 µM)
(23.5 h)
MCAo
reperfusion
euthanasia
90 min
30 min
MCA dissection
analysis of
angiogenic growth
(culture day 4, 5, 6,
7, 10 and 14)
B
WKY I/R
+ vehicle
+ uric acid 30 µM
Day 6
100 µm
100 µm
*
NS
Growth (µm)
Days of culture
I/R + vehicle
I/R + uric acid 10 µM
I/R + uric acid 30 µM
C
SHR I/R
+ vehicle
+ uric acid 30 µM
100 µm
100 µm
I/R + vehicle
I/R + uric acid 10 µM
I/R + uric acid 30 µM
*
Growth (µm)
Days of culture

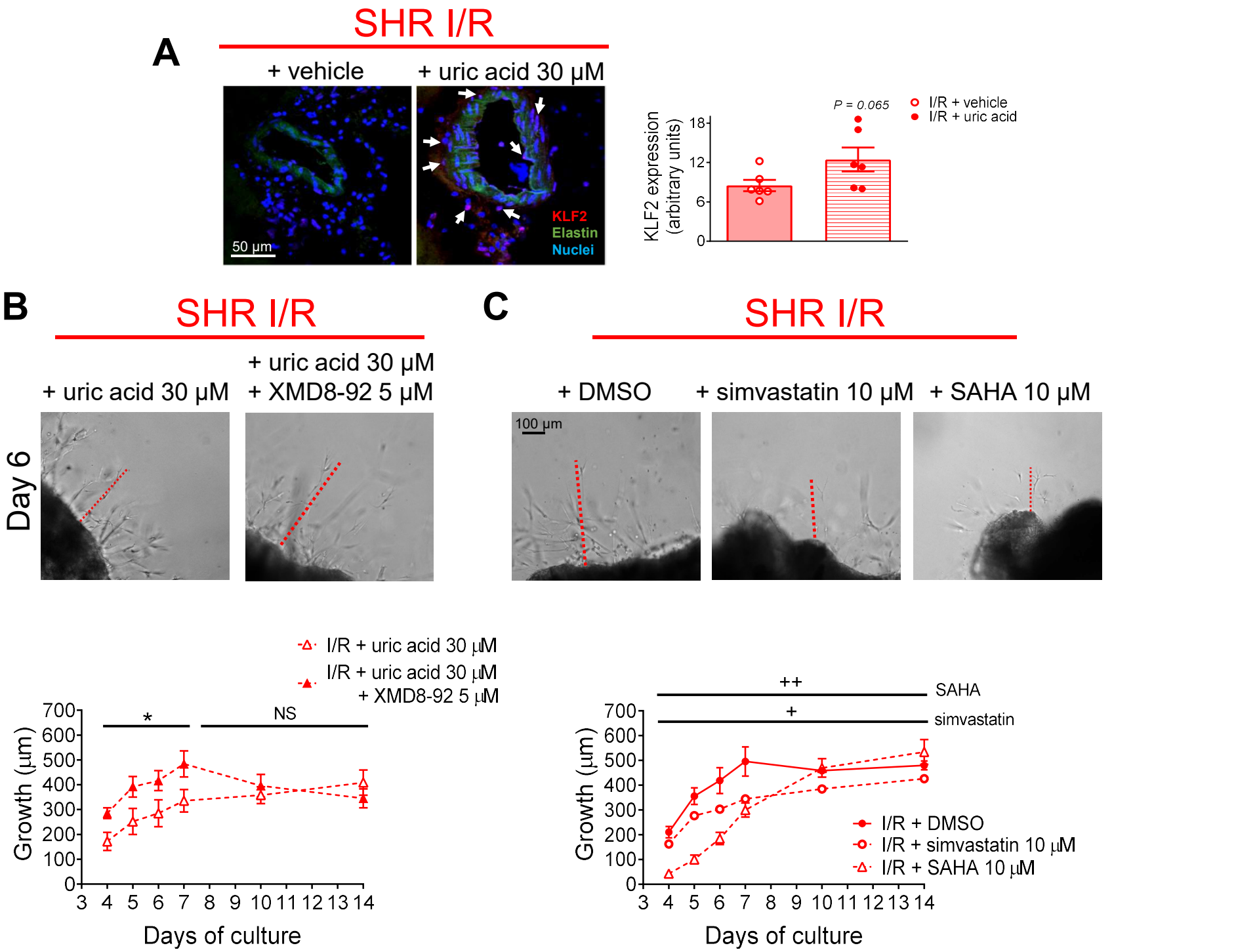
A
SHR I/R
+ vehicle
+ uric acid 30 µM
50 µm
KLF2
Elastin
Nuclei
P = 0.065
I/R + vehicle
I/R + uric acid
KLF2 expression (arbitrary units)
18
12
6
0
B
SHR I/R
+ uric acid 30 µM
+ uric acid 30 µM + XMD8-92 5 µM
Day 6
C
SHR I/R
+ DMSO
+ simvastatin 10 µM
+ SAHA 10 µM
100 µm
I/R + uric acid 30 µM
I/R + uric acid 30 µM + XMD8-92 5 µM
*
NS
Growth (µm)
Days of culture
++
+
SAHA
simvastatin
I/R + DMSO
I/R + simvastatin 10 µM
I/R + SAHA 10 µM

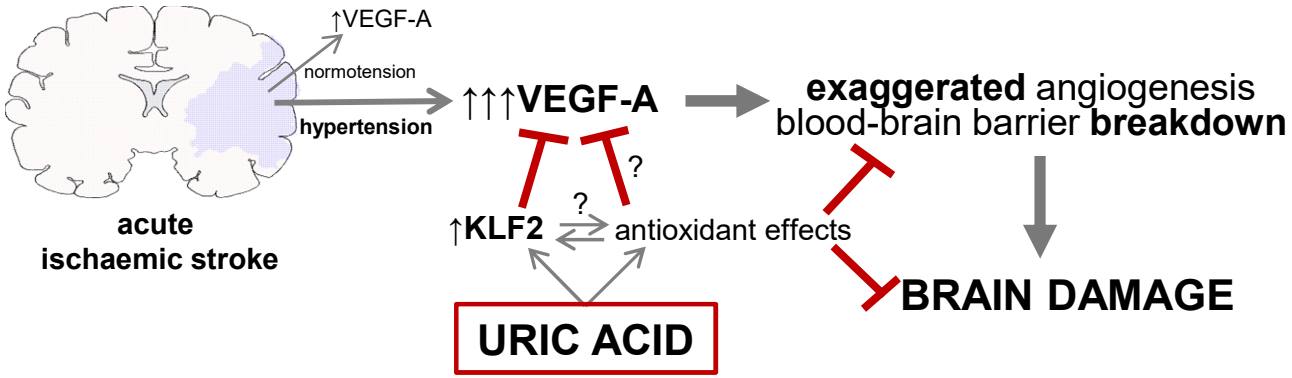
↑VEGF-A
normotension
hypertension
acute
ischaemic stroke
↑↑↑VEGF-A
?
?
↑KLF2
antioxidant effects
URIC ACID
exaggerated angiogenesis
blood-brain barrier breakdown
BRAIN DAMAGE